CHAPTER 22

SEAL TECHNOLOGY

Bruce M. Steinetz
NASA Lewis Research Center
Cleveland, Ohio

22.1 INTRODUCTION

Seals are required to fulfill critical needs in meeting the ever-increasing system-performance requirements of modern machinery. Approaching a seal design, one has a wide range of available seal choices. This chapter aids the practicing engineer in making an initial seal selection and provides current reference material to aid in the final design and application.

This chapter provides design insight and application for both static and dynamic seals. Static seals reviewed include gaskets, O-rings, and selected packings. Dynamic seals reviewed include mechanical face, labyrinth, honeycomb, and brush seals. For each of these seals, typical configurations, materials, and applications are covered. Where applicable, seal flow models are presented.

22.2 STATIC SEALS

22.2.1 Gaskets

Gaskets are used to effect a seal between two mating surfaces subjected to differential pressures. Gasket types and materials are limited only by one's imagination. Table 22.1 lists some common gasket materials and Table 22.2[1] lists common elastomer properties. The following gasket characteristics are considered important for good sealing performance.[2] Selecting the gasket material that has the best balance of the following properties will result in the best practical gasket design.

- Chemical compatibility
- Heat resistance
- Compressibility
- Microconformability (asperity sealing)
- Recovery
- Creep relaxation
- Erosion resistance
- Compressive strength (crush resistance)
- Tensile strength (blowout resistance)
- Shear strength (flange shearing movement)
- Removal or "Z" strength

Table 22.1   Common Gasket Materials, Gasket Factors (m) and Minimum Design Seating Stress (y) (Table 2-5.1 ASME Code for Pressure Vessels, 1995)
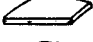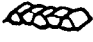
Gasket Material	Gasket Factor m	Min. Design Seating Stress y, psi	Sketches
Self-energizing types (O-rings, metallic, elastomer, other gasket types considered as self-sealing)	0	0	...
Elastomers without fabric or high percent of asbestos fiber:			
Below 75A Shore Durometer	0.50	0	
75A or higher Shore Durometer	1.00	200	
Asbestos with suitable binder for operating conditions:			
⅛ in. thick	2.00	1600	
1/16 in. thick	2.75	3700	
1/32 in. thick	3.50	6500	
Elastomers with cotton fabric insertion	1.25	400	
Elastomers with asbestos fabric insertion (with or without wire reinforcement):			
3-ply	2.25	2200	
2-ply	2.50	2900	
1-ply	2.75	3700	
Vegetable fiber	1.75	1100	
Spiral-wound metal, asbestos filled:			
Carbon	2.50	10,000	
Stainless, Monel, and nickel-base alloys	3.00	10,000	
Corrugated metal, asbestos inserted, or corrugated metal, jacketed asbestos filled:			
Soft aluminum	2.50	2900	
Soft copper or brass	2.75	3700	
Iron or soft steel	3.00	4500	
Monel or 4%–6% chrome	3.25	5500	
Stainless steels and nickel-base alloys	3.50	6500	
Corrugated metal:			
Soft aluminum	2.75	3700	
Soft copper or brass	3.00	4500	
Iron or soft steel	3.25	5500	
Monel or 4%–6% chrome	3.50	6500	
Stainless steels and nickel-base alloys	3.75	7600	

Table 22.1 *(Continued)*

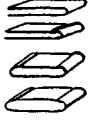| Gasket Material	Gasket Factor *m*	Min. Design Seating Stress *y*, psi	Sketches
Flat metal, jacketed asbestos filled:			
Soft aluminum	3.25	5500	
Soft copper or brass	3.50	6500	
Iron or soft steel	3.75	7600	
Monel	3.50	8000	
4%–6% chrome	3.75	9000	
Stainless steels and nickel-base alloys	3.75	9000	
Grooved metal:			
Soft aluminum	3.25	5500	
Soft copper or brass	3.50	6500	
Iron or soft steel	3.75	7600	
Monel or 4%–6% chrome	3.75	9000	
Stainless steels and nickel-base alloys	4.25	10,100	
Solid flat metal:			
Soft aluminum	4.00	8800	
Soft copper or brass	4.75	13,000	
Iron or soft steel	5.50	18,000	
Monel or 4%–6% chrome	6.00	21,800	
Stainless steels and nickel-base alloys	6.50	26,000	
Ring joint:			
Iron or soft steel	5.50	18,000	
Monel or 4%–6% chrome	6.00	21,800	
Stainless steels and nickel-base alloys	6.50	26,000	

- Antistick
- Heat conductivity
- Acoustic isolation
- Dimensional stability

Nonmetallic Gaskets. Most *nonmetallic gaskets* consist of a fibrous base held together with some form of an elastomeric binder. A gasket is formulated to provide the best load-bearing properties while being compatible with the fluid being sealed.

Nonmetallic gaskets are often reinforced to improve torque retention and blowout resistance for more severe service requirements. Some types of reinforcements include perforated cores, solid cores, perforated skins, and solid skins, each suited for specific applications. After a gasket material has been reinforced by either material additions or laminating, manufacturers can emboss the gasket raising a sealing lip, which increases localized pressures, thereby increasing sealability.

Metallic Gaskets. *Metallic gaskets* are generally used where either the joint temperature or load is extreme or in applications where the joint might be exposed to particularly caustic chemicals. A good seal capable of withstanding very high temperature is possible if the joint is designed to yield locally over a narrow location with application of bolt load. Some of the most common metallic gaskets range from soft varieties, such as copper, aluminum, brass, and nickel, to highly alloyed steels. Noble metals, such as platinum, silver, and gold, also have been used in difficult locations.

Metallic gaskets are available in both standard and custom designs. Since there is such a wide variety of designs and materials used, it is recommended that the reader directly contact metallic gasket suppliers for design and sealing information.

Required Bolt Load

ASME Method. The ASME Code for Pressure Vessels, Section VIII, Div. 1, App. 2, is the most commonly used design method for gasketed joints where important joint properties, including flange thickness, bolt size and pattern, are specified. Because of the absence of leakage considerations, it

should be noted that the ASME is currently evaluating the Pressure Vessel Research Council's method for gasket design. It is likely that a nonmandatory appendix to the Code will appear first (see discussion in Ref. 3).

An integral part of the AMSE Code revolves around two gasket factors:

1. An m factor, often called the gasket-maintenance factor, is associated with the hydrostatic end force and the operation of the joint.
2. The y factor is a rough measure of the minimum seating stress associated with a particular gasket material. The y factor pertains only to the initial assembly of the joint.

The ASME Code makes use of two basic equations to calculate bolt load, with the larger calculated load being used for design:

$$W_{m1} = H + H_p = \frac{\pi}{4} G^2 P + 2\pi b G m P$$

$$W_{m2} = H_y = \pi b G y$$

where W_{m1} = minimum required bolt load from maximum operating or working conditions, lb
W_{m2} = minimum required initial bolt load for gasket seating (atmospheric-temperature conditions) without internal pressure, lb
H = total hydrostatic end force, lb $[(\pi/4)G^2 P]$
H_p = total joint–contact–surface compression load, lb
H_y = total joint–contact–surface seating load, lb
G = diameter at location of gasket load reaction; generally defined as follows: When $b_0 <$ ¼ in., G = mean diameter of gasket contact face, in.; When $b_0 >$ ¼ in., G = outside diameter of gasket contact face less $2b$, in.
P = maximum internal design pressure, psi
b = effective gasket or joint–contact–surface *seating* width, in.
b = b_0 when $b_0 \leq$ ¼ in.
b = $0.5\sqrt{b_0}$ when $b_0 >$ ¼ in.
$2b$ = effective gasket or joint–contact–surface *pressure* width, in.
b_0 = basic gasket seating width per ASME Table 2-5.2. The table defines b_0 in terms of flange finish and type of gasket, usually from one-half to one-fourth gasket contact width
m = gasket factor per ASME Table 2-5.1 (repeated here as Table 22.1).
y = gasket or joint–contact–surface unit seating load, per ASME Table 2-5.1 (repeated here as Table 22.1), psi

The factor m provides a margin of safety to be applied when the hydrostatic end force becomes a determining factor. Unfortunately, this value is difficult to obtain experimentally since it is not a constant. The equation for W_{m2} assumes that a certain unit stress is required on a gasket to make it conform to the sealing surfaces and be effective. The second empirical constant y represents the gasket yield-stress value and is very difficult to obtain experimentally.

Practical Considerations

Flange Surfaces. Preparing the flange surfaces is paramount for effecting a good gasket seal. Surface finish affects the degree of sealability. The rougher the surface, the more bolt load required to provide an adequate seal. Extremely smooth finishes can cause problems for high operating pressures, as lower frictional resistance leads to a higher tendency for blowout. Surface finish lay is important in certain applications to mitigate leakage. Orienting finish marks transverse to the normal leakage path will generally improve sealability.

Flange Thickness. Flange thickness must also be sized correctly to transmit bolt clamping load to the area between the bolts. Maintaining seal loads at the midpoint between the bolts must be kept constantly in mind. Adequate thickness is also required to minimize the bowing of the flange. If the flange is too thin, the bowing will become excessive and no bolt load will be carried to the midpoint, preventing sealing.

Bolt Pattern. Bolt pattern and frequency are critical in effecting a good seal. The best bolt clamping pattern is invariably a combination of the maximum practical number of bolts, optimum spacing, and positioning.

One can envision the bolt loading pattern as a series of straight lines drawn from bolt to adjacent bolt until the circuit is completed. If the sealing areas lie on either side of this pattern, it will likely be a potential leakage location. Figure 22.1 shows an example of the various conditions.[2] If bolts
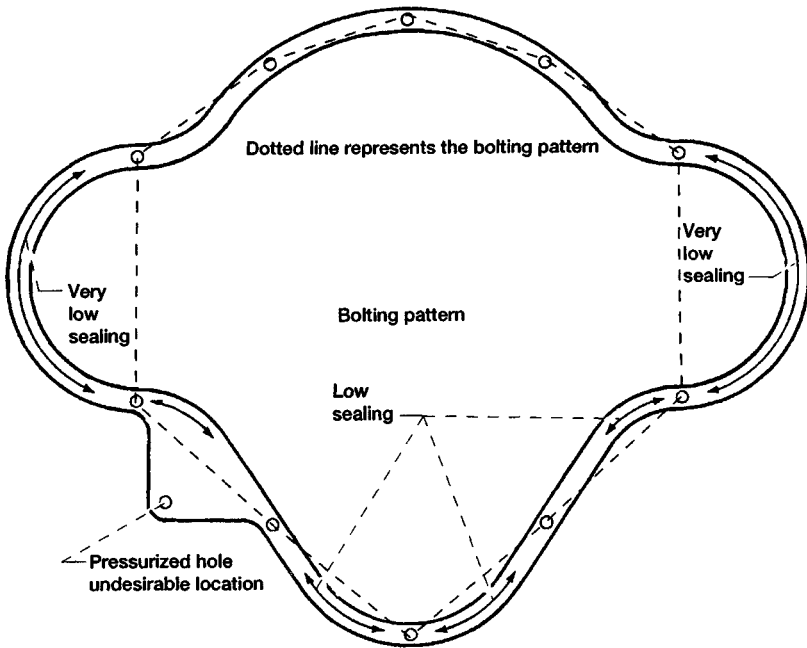
Fig. 22.1   Bolting pattern indicating poor sealing areas. (From Ref. 2.)

cannot be easily repositioned on a problematic flange, Fig. 22.2 illustrates techniques to improve gasket effectiveness through reducing gasket face width where bolt load is minimum. Note that gasket width is retained in the vicinity of the bolt to support local bolt loads and minimize gasket tearing.

Gasket Thickness and Compressibility.   Gasket thickness and compressibility must be matched to the rigidity, roughness, and unevenness of the mating flanges. An effective gasket seal is achieved only if the stress level imposed on the gasket at installation is adequate for the specific gasket and joint requirements.
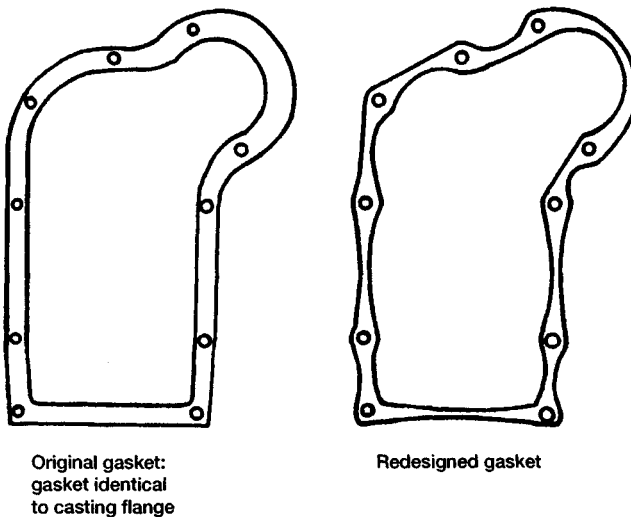
Fig. 22.2   Original vs. redesigned gasket for improved sealing. (From Ref. 2.)

Gaskets made of compressible materials should be as thin as possible. Adequate gasket thickness is required to seal and conform to the unevenness of the mating flanges, including surface finish, flange flatness, and flange warpage during use. A gasket that is too thick can compromise the seal during pressurization cycles and is more likely to exhibit creep relaxation over time.

22.2.2 O-Rings

O-ring seals are perhaps one of the most common forms of seals. Following relatively straightforward design guidelines, a designer can be confident of a high-quality seal over a wide range of operating conditions. This section provides useful insight to designers approaching an O-ring seal design, including basic sealing mechanism, preload, temperature effects, common materials, and chemical compatibility with a range of working fluids. The reader is directed to manufacturer's design manuals for detailed information on the final selection and specification.[4]

#### Basic Sealing Mechanism

O-rings are compressed between the two mating surfaces and are retained in a seal gland. The initial compression provides initial sealing critical to successful sealing. Upon increase of the pressure differential across the seal, the seal is forced to flow to the lower pressure side of the gland (see Fig. 22.3). As the seal moves, it gains greater area and force of sealing contact. At the pressure limit of the seal, the O-ring just begins to extrude into the gap between the inner and outer member of the gap. If this pressure limit is exceeded, the O-ring will fail by extruding into the gap. The shear strength of the seal material is no longer sufficient to resist flow and the seal material extrudes (flows) out of the open passage. Back-up rings are used to prevent seal extrusion for high-pressure static and for dynamic applications.

Preload

The tendency of an O-ring to return to its original shape after the cross section is compressed is the basic reason why O-rings make such excellent seals. The maximum linear compression suggested by manufacturers is 30% for static applications and 16% for dynamic seals (up to 25% for small cross-sectional diameters). Compression less than these values is acceptable, within reason, if assembly
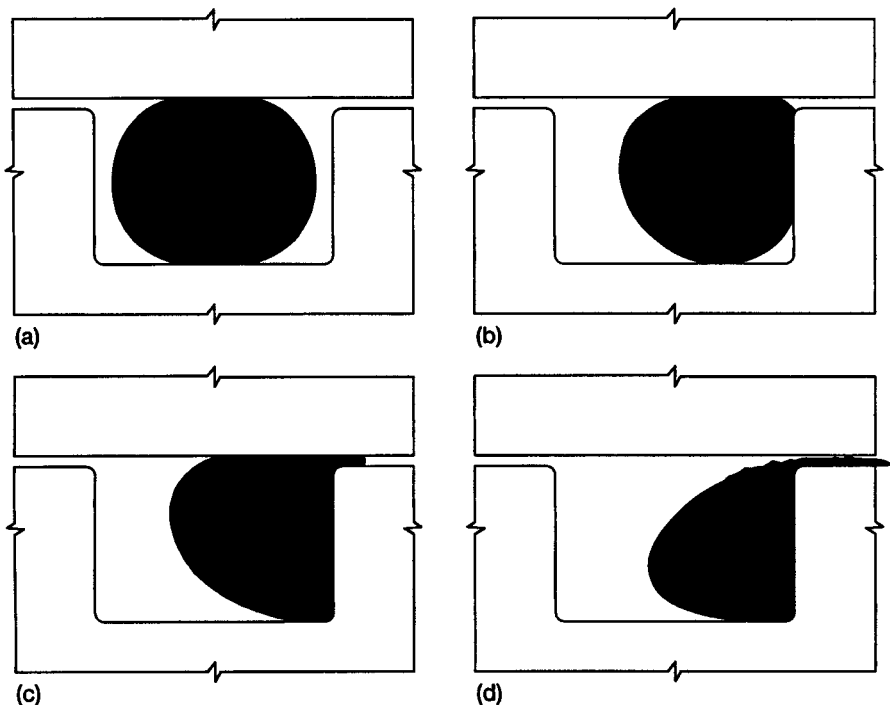

Fig. 22.3 Basic O-ring sealing mechanism. (a) O-ring installed; (b) O-ring under pressure;
(c) O-ring extruding; (d) O-ring failure. (From Ref. 4.)

problems are an issue. Manufacturers recommend[4] a minimum amount of initial linear compression to overcome compression set that O-rings exhibit.

O-ring compression force depends principally on the hardness of the O-ring, its cross-sectional dimension, and the amount of compression. Figure 22.4 illustrates the range of compressive force per linear inch of seal for typical linear percent compressions (0.139 in. cross-section diameter) and compound hardness (Shore A hardness scale). Softer compounds provide better sealing ability, as the rubber flows more easily into the grooves. Harder compounds are specified for high pressures, to limit chance of extruding into the groove, and to improve wear life for dynamic service. For most applications, compounds having a Type A durometer hardness from 70–80 are the most suitable compromise.[4]

Thermal Effects

O-ring seals respond to temperature changes. Therefore, it is critical to ensure the correct material and hardness is selected for the application. High temperatures soften compounds. This softening can negatively affect the seal's extrusion resistance at temperature. Over long periods of time at high temperature, chemical changes occur. These generally cause an increase in hardness, along with volume and compression-set changes.

O-ring compounds harden and contract at cold temperatures. These effects can both lead to a loss of seal if initial compression is not set properly. Because the compound is harder, it does not flow into the mating surface irregularities as well. Just as important, the more common O-ring materials have a coefficient of thermal expansion 10 times greater than that of steel (i.e., nitrile CTE is 6.2×10^{-5}°F).

Groove dimensions must be sized correctly to account for this dimensional change. Manufacturers design charts[4] are devised such that proper O-ring sealing is ensured for the temperature ranges for standard elastomeric materials. However, the designer may want to modify gland dimensions for a given application that experiences only high or low temperatures in order to maintain a particular squeeze on the O-ring. Martini[5] gives several practical examples showing how to tailor groove dimensions to maintain a given squeeze for the operating temperature.

Material Selection/Chemical Compatibility

Seal compounds must work properly over the required temperature range, have the proper hardness to resist extrusion while effectively sealing, and must also resist chemical attack and resultant swelling caused by the operating fluids. Table 22.2 summarizes the most important elastomers, their working temperature range, and their resistance to a range of common working fluids.

Rotary Applications

O-rings are also used to seal rotary shafts where surface speeds and pressures are relatively low. One factor that must be carefully considered when applying O-ring seals to rotary applications is the Gow-
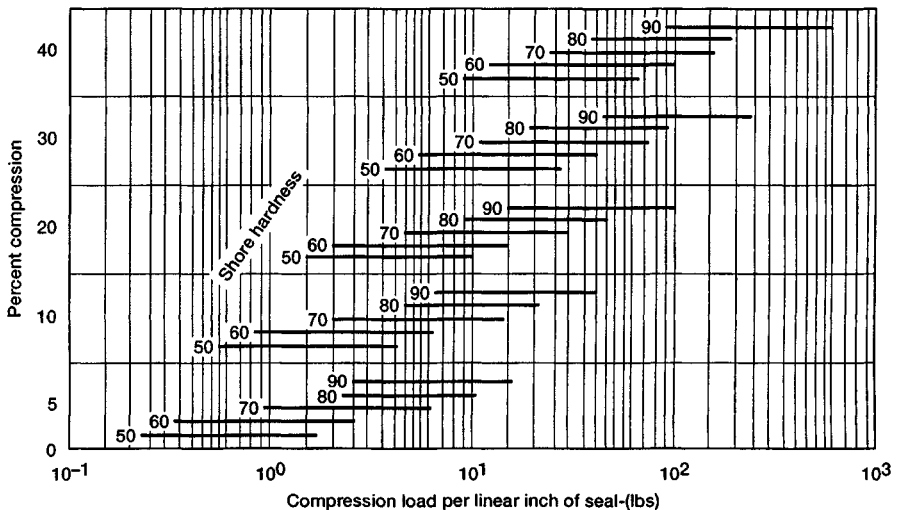

Fig. 22.4 Effect of percent compression and material Shore hardness on seal compression load, 0.139-in. cross section. (From Ref. 4.)

Table 22.2 The Most Important Elastomers and Their Properties[1]

Elastomer	Composition	Working temperature range, °C	Tensile strength, bar	Elongation, %	Hardness, °Shore	Water	Steam	Hydraulic fluids, non-flammable (ester-based)	Mineral fats and oils	Vegetable and animal fats and oils	Ozone	Aliphatic	Aromatic	Halogenated	Alcohols	Ketones	Esters	Dilute acids	Concentrated acids	Dilute alkalis	Concentrated alkalis	Saline solutions
												Hydrocarbons										
Natural rubber	Rubber, K. W. Coil Refining-type polymerisate	−30 to 120	50 to 280	1000	30 to 98	x	x	—	—	—	—	—	—	—	x	x	—	o	—	x	o	x
S.B.R.	Butadiene–styrene copolymer	−30 to 130	50 to 240	700	40 to 95	x	x	—	—	—	o	—	—	—	x	x	—	x	o	x	x	x
Nitrile N	Butadiene–acrylonitrile copolymer	−30 to 130	50 to 240	700	40 to 95	x	o	—	x	x	o	x	o	—	x	—	—	o	—	o	o	x
Neoprene	Chlorinated–butadiene polymerisate	−40 to 140	50 to 270	800	40 to 95	x	x	—	o	o	x	o	—	—	x	—	—	x	o	x	x	x
Butyl	Isobutylene–isoprene copolymer	−50 to 150	40 to 170	900	40 to 90	x	x	o	—	o	x	—	o	—	x	o	o	x	o	x	x	x
Hypalon	Chloro–sulfonated polyethylene	−40 to 140	40 to 200	600	40 to 95	x	o	—	—	o	x	—	—	—	x	—	—	x	o	x	x	x
Silicone rubber	Polycondensates of dialkylsiloxanes	−100 to 200	20 to 80	500	40 to 80	o	—	—	o	x	x	o	—	—	x	o	—	x	o	x	o	o
Thiokol	Alkylopolysulfide	−40 to 80	10 to 60	200	65 to 80	x	—	x	x	x	x	x	o	o	x	o	x	x	o	x	x	x
Polyacrylic	Polyacrylate	−30 to 120	20 to 70	700	70 to 85	o	—	x	x	x	x	x	o	o	o	—	x	—	—	o	—	o
Vulcollan	Polyurethane	−30 to 80	200 to 320	600	70 to 95	o	—	—	x	x	x	x	—	—	o	—	—	—	—	—	—	—
Adiprene	Polyurethane	−40 to 120	80 to 300	700	70 to 95	x	o	—	x	x	x	x	—	—	o	—	—	—	—	—	—	—
Kel-F	Copolymer of chlorotriethylene and vinylidene fluoride	−50 to 180	30 to 120	700	60 to 90	x	x	—	—	o	x	o	—	—	x	—	—	x	x	x	x	x
Viton	Vinylidene fluoride–hexafluoropropylene copolymer	−60 to 200	80 to 160	300	60 to 95	x	o	o	x	x	x	x	x	o	x	—	—	x	o	o	—	x
PTFE	Polytetrafluoroethylene	−200 to 280	140 to 310	200	55D	x	x	x	x	x	x	x	x	x	x	x	x	x	x	x	x	x
E.P.R.	Ethylene–propylene	−55 to 200	50 to 160	400	70 to 95	x	x	x	—	—	x	—	—	—	x	x	o	x	o	x	x	x
F.S.R.	Fluoro–silicone rubber	−60 to 230	55 to 85	400	40 to 80	o	o	o	x	x	x	x	x	o	x	—	o	o	—	x	o	x

Note: x, stable; o, stable under certain conditions; —, unstable.

Joule effect.[5] When a rubber O-ring is stretched slightly around a rotating shaft, (e.g. put in tension) friction between the ring and shaft generates heat causing the ring to contract, exhibiting a negative expansion coefficient. As the ring contracts friction forces increase generating additional heat and further contraction. This positive-feedback cycle causes rapid seal failures. Similar failures in reciprocating applications and static applications are unusual because surface speeds are too low to initiate the cycle. Further, in reciprocating applications the seal is moved into contact with cooler adjacent material. To prevent the failure cycle, O-rings are not stretched over shafts but are oversized slightly (circumferentially) and compressed into the sealing groove. The pre-compression of the cross-section results in O-ring stresses that oppose the contraction stress preventing the failure cycle described. Martini[5] provides guidelines for specifying the O-ring seal. Following appropriate techniques O-ring seals have run for significant periods of time at speeds up to 750 fpm and pressures up to 200 psi.

22.2.3 Packings and Braided Rope Seals

Rope packings used to seal stuffing boxes and valves and prevent excessive leakage can be traced back to the early days of the Industrial Revolution. An excellent summary of types of rope seal packings is given in Ref. 6. Novel adaptations of these seal packings have been required as temperatures have continued to rise to meet modern system requirements. New ceramic materials are being investigated to replace asbestos in a variety of gasket and rope-packing constructions.

Materials

Packing materials are selected for intended-temperature and chemical environment. Graphite-based packing/gaskets are rated for up to 1000°F for oxidizing environments and up to 5400°F for reducing environments.[7] Used within its recommended temperature, graphite will provide a good seal with acceptable ability to track joint movement during temperature/pressure excursions. Graphite can be laminated with itself to increase thickness or with metal/plastic to improve handling and mechanical strength. Table 22.2 provides working temperatures for conventional (e.g., nitrile, PTFE, neoprene, amongst others) gasket/packings. Table 22.3 provides typical maximum working temperatures for high temperature gasket/packing materials.

Packings and Braided Rope Seals for High-Temperature Service

High-temperature packings and rope seals are required for a variety of applications, including sealing: furnace joints, locations within continuous casting units (gate seals, mold seals, runners, spouts, etc.), amongst others. High-temperature packings are used for numerous aerospace applications, including turbine casing and turbine engine locations, Space Shuttle thermal protection systems, and nozzle joint seals.

Aircraft engine turbine inlet temperatures and industrial system temperatures continue to climb to meet aggressive cycle thermal efficiency goals. Advanced material systems, including monolithic/composite ceramics, intermetallic alloys (i.e., nickel aluminide), and carbon–carbon composites, are

Table 22.3   Gasket/Rope Seal Materials

Fiber Material	Maximum Working Temperature °F
Graphite	
Oxidizing environment	1000
Reducing	5400
Fiberglass (glass dependent)	1000
Superalloy metals	
(depending on alloy)	1300–1600
Oxide Ceramics (Ref. Tompkins 1995)*	
62% Al_2O_3 24% SiO_2 14% B_2O_3 (Nextel 312)	1800†
70% Al_2O_3 28% SiO_2 2% B_2O_3 (Nextel 440)	2000†
73% Al_2O_3 27% SiO_2 (Nextel 550)	2100†

*Tompkins, T. L. "Ceramic Oxide Fibers: Building Blocks for New Applications," Ceramic Industry Publ, Business News Publishing, April, 1995.
†Temperature at which fiber retains 50% (nominal) room temperature strength.

being explored to meet aggressive temperature, durability, and weight requirements. Incorporating these materials in the high-temperature locations in the system, designers must overcome materials issues, such as differences in thermal expansion rates and lack of material ductility.

Designers are finding that one way to avoid cracking and buckling of the high-temperature brittle components rigidly mounted in their support structures is to allow relative motion between the primary and supporting components.[8] Often this joint occurs in a location where differential pressures exist, requiring high-temperature seals. These seals or packings must exhibit the following important properties: operate hot ($\geq$1300°F); exhibit low leakage; resist mechanical scrubbing caused by differential thermal growth and acoustic loads; seal complex geometries; retain resilience after cycling; and support structural loads.

In an industrial seal application, a high-temperature all-ceramic seal is being used to seal the interface between a low-expansion rate primary structure and the surrounding support structure. The seal consists of a dense uniaxial fiber core overbraided with two two-dimensional braided sheath layers.[8] Both core and sheath are composed of 8 μm alumina–silica fibers (Nextel 550) capable of withstanding 2000+°F temperatures. In this application over a heat/cool cycle, the support structure moves 0.3 in. relative to the primary structure, precluding normal fixed-attachment techniques. Leakage flows for the all-ceramic seal are shown in Fig. 22.5 for three temperatures after simulated scrubbing[8] (10 cycles $\times$ 0.3-in. at 1300°F).

In a turbine vane application, the conventional braze joint is replaced with a floating seal arrangement incorporating a small-diameter (1/16-in.) rope seal (Fig. 22.6). The seal is designed to serve as a seal and a compliant mount, allowing relative thermal growth between the high-temperature turbine vane and the lower-temperature support structure, preventing thermal strains and stresses. A hybrid seal consisting of a dense uniaxial ceramic core (8 μm alumina–silica Nextel 550 fibers) overbraided with a superalloy wire (0.0016-in. diameter Haynes 188 alloy) abrasion-resistant sheath has proven successful for this application.[9] Leakage flows for the hybrid seal are shown in Fig. 22.7 for two temperatures, and pressures under two preload conditions after simulated scrubbing (10 cycles $\times$ 0.3-in. at 1300°F).

Recent studies[8] have shown the benefits of high sheath braid angle and double-stage seals for reducing leakage. Increasing hybrid seal sheath braid angle and increasing core coverage led to increased compressive force (for the same linear seal compression) and one-third the leakage of the conventional hybrid design. Adding a second seal stage reduced seal leakage 30% relative to a single stage.

22.3 DYNAMIC SEALS

22.3.1 Initial Seal Selection

An engineer approaching a dynamic seal design has a wide range of seals to choose from. A partial list of seals available ranges from the mechanical face seal through the labyrinth and brush seal, as
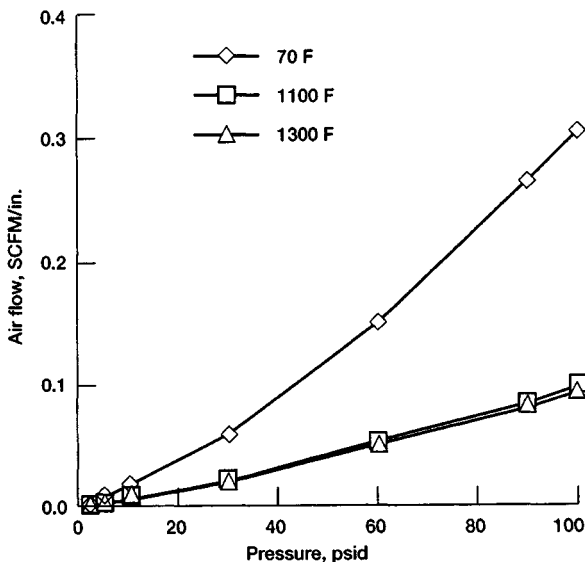

Fig. 22.5 Flow vs. pressure data for 3 temperatures, 1/16 in. diameter all-ceramic seal, 0.022 in. seal compression, after scrubbing. (From Ref. 8.)
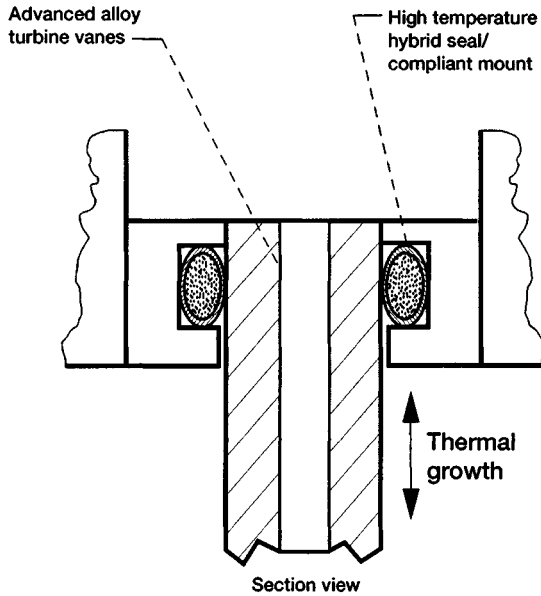
Fig. 22.6 Schematic of turbine vane seal. (From Ref. 9.)

indicated in Fig. 22.8. To aid in the initial seal selection, a "decision tree" has been proposed by Fern and Nau.[10] The decision tree (see Fig. 22.9) has been updated for the current work to account for the emergence of brush seals. In this chart, a majority of answers either "yes" or "no" to the questions at each stage leads the designer to an appropriate seal starting point. If answers are equally divided, both alternatives should be explored using other design criteria, such as performance, size, and cost.

The scope of this chapter does not permit treatment of every entry in the decision tree. However, several examples are given below to aid in understanding its use.

Radial lip seals are used to prevent fluids, normally lubricated, from leaking around shafts and their housings. They are also used to prevent dust, dirt, and foreign contaminants from entering the
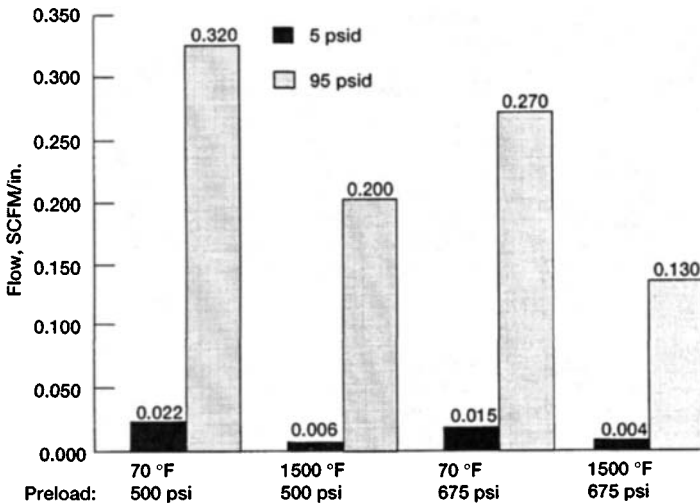

Fig. 22.7 The effect of temperature, pressure, and representative compression on seal flow after cycling for 0.060-in. hybrid vane seal. (From Ref. 9.)
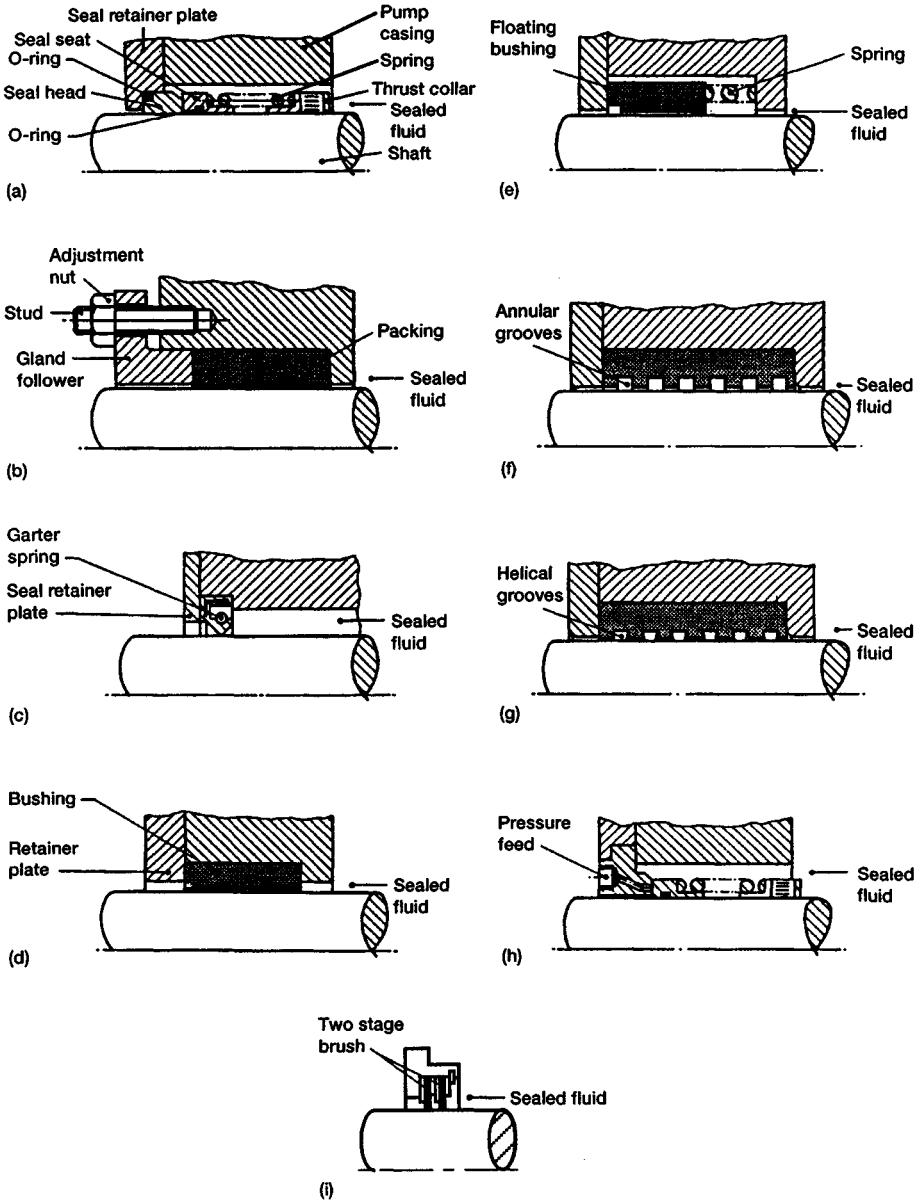
Fig. 22.8 Examples of the main types of rotary seal. (a) Mechanical face seal; (b) Stuffing box; (c) Lip seal; (d) Fixed bushing; (e) Floating bushing; (f) Labyrinth; (g) Viscoseal; (h) Hydrostatic seal; (i) Brush seal. ((a)–(h) From Ref. 10.)

lubricant chamber. Depending on conditions, lip seals have been designed to operate at very high shaft speeds (6,000–12,000 rpm) with light oil mist and no pressure in a clean environment. Lip seals have replaced mechanical face seals in automotive water pumps at pressures to 30 psi, temperatures −45°F to 350°F, and shaft speeds to 8000 sfpm (American Variseal, 1994). Lip seals are also used in completely flooded low-speed applications or in muddy environments. A major advantage of the radial lip seal is its compactness. A 0.32-in. by 0.32-in. lip seal provides a very good seal for a 2-in. diameter shaft.

Mechanical face seals are capable of handling much higher pressures and a wider range of fluids. Mechanical face seals are recommended over brush seals where very high pressures must be sealed
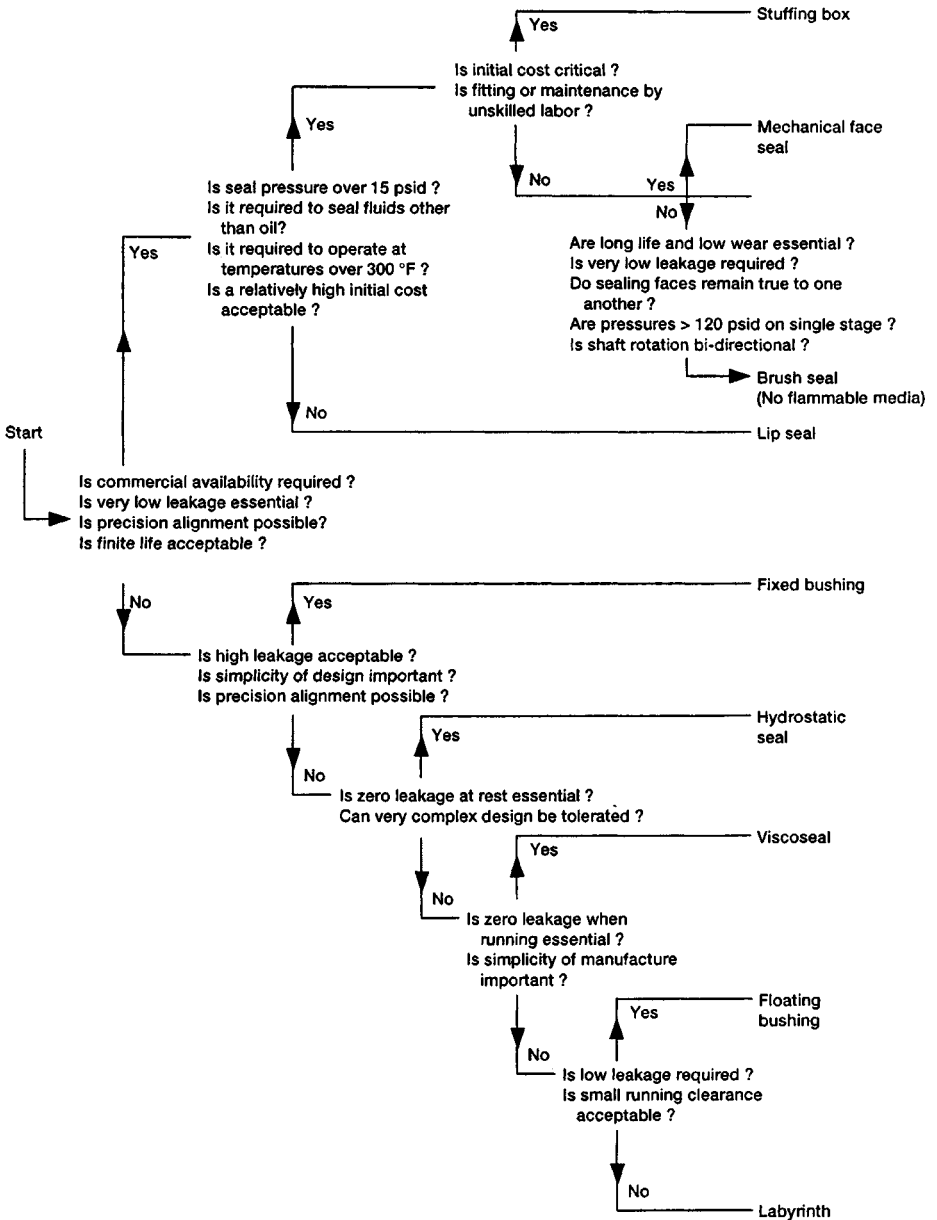
Fig. 22.9 Seal selection chart (a majority answer of "yes" or "no" to the question at each stage leads the reader to the appropriate decision; if answers are equally divided both alternatives should be explored). (Adapted from Ref. 10.)

in a single stage. Mechanical face seals have a lower leakage than brush seals because their effective clearances are several times smaller. However, the mechanical face seal requires much better control of dimensions and tolerates less shaft misalignment and runout, thereby increasing costs.

Turbine Engine Seals. Readers interested particularly in turbine engine seals are referred to Steinetz and Hendricks,[11] (1997) which reviews in greater depth the tradeoffs in selecting seals for turbine engine applications. Technical factors increasing seal design complexity for aircraft engines include high temperatures ($\geq 1000°F$), high surface speeds (up to 1500 fps), rapid thermal/structural transients, maneuver and landing loads, and the requirement to be lightweight.

22.3.2 Mechanical Face Seals

The primary elements of a conventional spring-loaded mechanical face seal are the primary seal (the main sealing faces), the secondary seal (seals shaft leakage), and the spring or bellows element that keep the primary seal surfaces in contact, shown in Fig. 22.8. The primary seal faces are generally lapped to demanding surface flatness, with surface flatness of 40 μin (1 micron) not uncommon. Surface flatness this low is required to make a good seal, since the running clearances are small. Conventional mechanical face seals operate with clearances of 40–200 μin. Dry-running, noncontacting gas face seals that use spiral groove face geometry reliably run at pressures of 1800 psig and speeds up to 590 fps (John Crane, 1993).

Seal Balance

Seal balancing is a technique whereby the primary seal front and rear areas are used to minimize the contact pressure between the mating seal faces to reduce wear and to increase the operating pressure capability. The concept of seal balancing is illustrated in Fig. 22.10.[12] The front and rear faces of the seal in Fig. 22.10a are identical and the full fluid pressure exerted on A' is carried on the seal face A. By modifying the geometry of the primary seal head ring to establish a smaller frontal area A' (Fig. 22.10b) and to provide a shoulder on the opposite side of the seal ring to form a front face B', the hydraulic pressure counteracts part of the hydraulic loading from A'. Consequently, the remaining face pressure in the contact interface is significantly reduced. Depending on the relative sizes of surfaces A' and B', the seal is either partially balanced (Fig. 22.10b) or fully balanced (Fig. 22.10c). In fully balanced seals, there is no net hydraulic load exerted on the seal face. Seals are
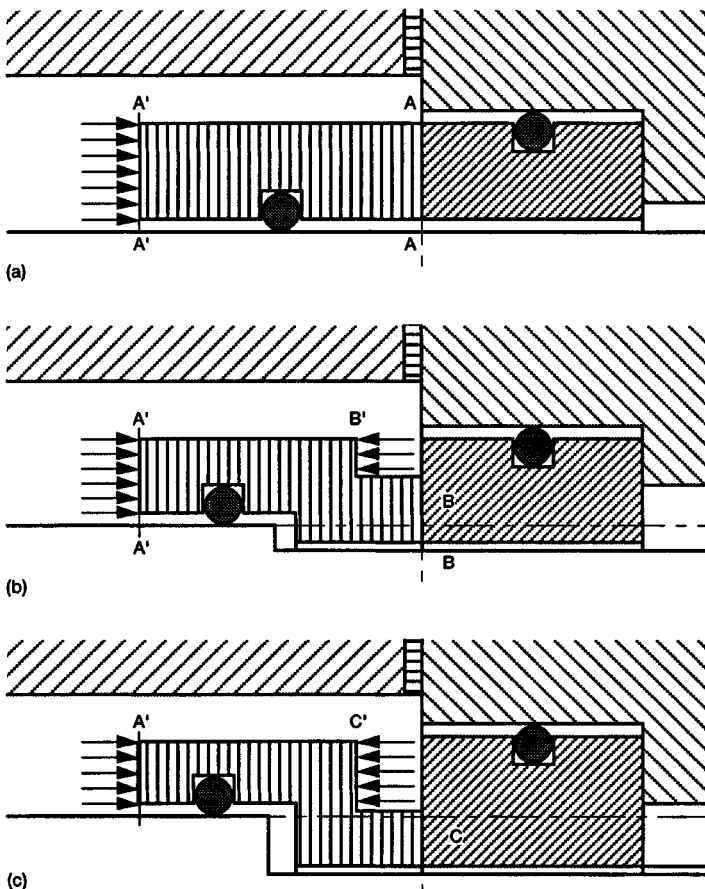

Fig. 22.10 Illustration of face seal balance conditions. (a) Unbalanced; (b) Partially balanced; (c) Fully balanced. (From Ref. 12.)

generally run with a partial balance, however, to minimize face loads and wear while keeping the seal closed during possible transient overpressure conditions. Partially balanced seals can run at pressures greater than six times unbalanced seals can for the same speed and temperature conditions.

Mechanical Face Seal Leakage

Liquid Flow. Minimizing leakage between seal faces is possible only through maintaining small clearances. Volumetric flow (Q) can be determined for the following two conditions (Lebeck, 1991).[13]

For Coned Faces:

$$Q = \frac{\pi \phi r_m}{3\mu} \left(\frac{P_o - P_i}{1/h_o^2 - 1/h_i^2} \right)$$

For Parallel Faces:

$$Q = \frac{-\pi r_m h^3}{6\mu} \frac{(P_o - P_i)}{(r_o - r_i)} \qquad h_o = h_i \quad \text{and} \quad ((r_o - r_i)/r_m < 0.1)$$

where ϕ (radians) is the cone angle (positive if faces are convergent travelling inward radially); r_o, r_i (in.) outer and inner radii; r_m (in.) mean radius (in.); h_o, h_i (in.) outer and inner film thicknesses; P_o, P_i (psi) outer and inner pressures; μ (lbf $\cdot$ s/in.²) viscosity. The need for small clearances is demonstrated by noting that doubling the film clearance, h, increases the leakage flow eight-fold.

Gas Flow. Closed-form equations for gas flow through parallel faces can be written only for conditions of laminar flow (Reynolds No. < 2300). For laminar flow with a parabolic pressure distribution across the seal faces, the mass flow is given as (Lebeck, 1991):[13]

$$\dot{m} = \frac{\pi r_m h^3}{12\mu RT} \frac{(P_i^2 - P_o^2)}{(r_o - r_i)} \qquad (r_o - r_i)/r_m < 0.1$$

where R is the gas constant (53.3 lbf $\cdot$ ft/lb$_m$ $\cdot$ °R for air), and T (°R) is the gas temperature (isothermal throughout).

In cases where flow is both laminar and turbulent, iterative schemes must be employed. See Refs. 13 and 14 for numerical algorithms to use in solving for the seal leakage rates. Reference 15 treats the most general case of two-phase flow through the seal faces.

Seal Face Flatness

In addition to lapping faces to the 40 μin. flatness, there are several other points to consider. The lapped rings should be mounted on surfaces that are themselves flat. The ring must be stiff enough to resist distortions caused either by thermal or fluid pressure stresses.

The primary mode of distortion of a mechanical seal face under combined fluid and thermal stresses is solid body rotation about the seal's neutral axis.[10] If the sum of the moments M (in.-lb/in.) per unit of circumference around the neutral axis can be calculated, then the angular deflection θ (radians) of the sealing face, can be obtained from

$$\theta = Mr_m^2/EI$$

where E (psi) = Young's modulus
  I (in.⁴) = the second moment of areas about the neutral axis
  r_m (in.) = the mean radius of the seal ring

Face Seal Materials

Selecting the correct materials for a given seal application is critical to ensuring desired performance and durability. Seal components for which material selection is important from a tribology standpoint are the stationary nosepiece (or primary seal ring) and the mating ring (or seal seat). Properties considered ideal for the primary seal ring are shown below.[16]

1. Mechanical:
   (a) High modulus of elasticity
   (b) High tensile strength
   (c) Low coefficient of friction
   (d) Excellent wear characteristics and hardness
   (e) Self-lubrication

  2. Thermal:
    (a) Low coefficient of expansion
    (b) High thermal conductivity
    (c) Thermal shock resistance
    (d) Thermal stability
  3. Chemical:
    (a) Corrosion resistance
    (b) Good wetability
  4. Miscellaneous:
    (a) Dimensional stability
    (b) Good machinability and ease of manufacture
    (c) Low cost and ready availability

Carbon–graphite is often the first choice for one of the running seal surfaces because of its superior dry-running (i.e., start-up) behavior. It can run against itself, metals, or ceramics without galling or seizing. Carbon–graphite is generally impregnated with resin or with a metal to increase thermal conductivity and bearing characteristics. In cases where the seal will see considerable abrasives, carbon may wear excessively and then it is desirable to select very hard seal-face materials. A preferred combination for very long wear (subject to other constraints) is tungsten carbide running on tungsten carbide. For a comprehensive coverage of face seal material selection, including chemical compatibility, see Ref. 17.

    Secondary seals are either O-rings or bellows. Temperature ranges and chemical compatibility for common O-ring secondary seals such as nitrile, fluorocarbon (Viton), and PTFE (Teflon) are provided in Table 22.2.

22.3.3 Emission Concerns

Mechanical face seals have played and will continue to play a major role for many years in minimizing emissions to the atmosphere. New federal, state, and local environmental regulations have intensified the focus on mechanical face seal performance in terms of emissions. Within a short time, regulators have gone from little or no concern about fugitive hazardous emissions to a position of severely restricting all hazardous emissions. For instance, under the authority of Title III of the 1990 Clean Air Act Amendment (CAAA), the U.S. Environmental Protection Agency (EPA) adopted the National Emission Standards for Hazardous Air Pollutants (NESHAP) for the control of emissions of volatile hazardous air pollutants (Ref. STLE, 1994).[18] Leak definition per the regulation (EPA HON Subpart H (5)) are defined as follows:

    Phase I: 10,000 parts per million volumetric (ppmv), beginning on compliance date
    Phase II: 5000 ppmv, 1 year after compliance date
    Phase III: 1000–5000 ppmv, depending on application, 2½ years after compliance date

    The Clean Air Act regulations require U.S. plants to reduce emissions of 189 hazardous air pollutants by 80% in the next several years.[19] The American Petroleum Industry (API) has responded with a standard of its own, known as API 682, that seeks to reduce maintenance costs and control volatile organic compounds (VOC) emissions on centrifugal and rotary pumps in heavy service. API 682, a pump shaft sealing standard, is designed to help refinery pump operators and similar users comply with environmental emissions regulations. These regulations will continue to have a major impact on users of valves, pumps, compressors and other processing devices. Seal users are cautioned to check with their state and local air quality control authorities for specific information.

Sealing Approaches for Emissions Controls

The Society of Tribologists and Lubrication Engineers published a guideline of mechanical seals for meeting the fugitive emissions requirements.[18] Seal technology available meets approximately 95% of current and anticipated federal, state, and local emission regulations. Applications not falling within the guidelines include food, pharmaceutical, and monomer-type products where dual seals cannot be used because of product purity requirements and chemical reaction of dual seal buffer fluids with the sealed product.

    Three sealing approaches for meeting the new regulatory requirements are discussed below: single seals, tandem seals, and double seals.[18]

    Single Seals. The most economical approach available is the single seal mounted inside a stuffing box (Fig. 22.11). Generally, this type of seal uses the pumped product for lubrication. Due to some finite clearance between the faces, there is a small amount of leakage to atmosphere. Using current technology in the design of a single seal, emissions can be controlled to 500 ppm based on
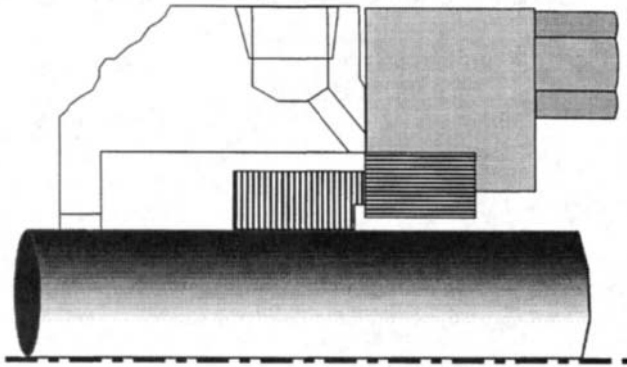
Fig. 22.11 Single seal. (From Ref. 18.)

both laboratory and field test data. Emission to atmosphere can be eliminated by venting the atmospheric side to a vapor recovery or disposal system. Using this approach, emissions readings approaching zero can be achieved. Since single seals have a minimum of contacting parts and normally require minimum support systems, they are considered highly reliable.

Tandem Seals. Tandem seals consist of two seal assemblies between which a barrier fluid operates at a pressure less than the pumped process pressure. The inboard primary seal seals the full pumped product pressure, and the outboard seal typically seals a nonpressurized barrier fluid (Fig. 22.12). Tandem seal system designs are available that provide zero emission of the pumped product to the environment, provided the vapor pressure of the product is higher than that of the barrier fluid and the product is immiscible in the barrier fluid. The barrier fluid isolates the pumped product from the atmosphere and is maintained by a support system. This supply system generally includes a supply tank assembly and optional cooling system and means for drawing off the volatile component (generally at the top of the supply tank). Examples of common barrier fluids are found in Table 22.4.

Tandem seal systems also provide a high level of sealing and reliability, and are simple systems to maintain, due to the typical use of nonpressurized barrier fluid. Pumped product contamination by the barrier fluid is avoided since the barrier fluid is at a lower pressure than the pumped product.

Double Seals. Double seals differ from tandem seals in that the barrier fluid between the primary and outboard seal is pressurized (Fig. 22.13). Double seals can be either externally or internally pressurized. An externally pressurized system requires a lubrication unit to pressurize the barrier fluid above the pumped product pressure and to provide cooling. An internally pressurized double seal refers to a system that internally pressurizes the fluid film at the inboard faces as the shaft rotates. In this case, the barrier fluid in the seal chamber is normally at atmospheric pressure. This results in less heat generation from the system.

Application Guide. The areas of application based on emissions to atmosphere for the three types of seals discussed are illustrated in Fig. 22.14. The scope of this chart is for seals less than 6 in. in diameter, for pressures 600 psig and less, and for surface speeds up to 5600 fpm. Waterbury[19]
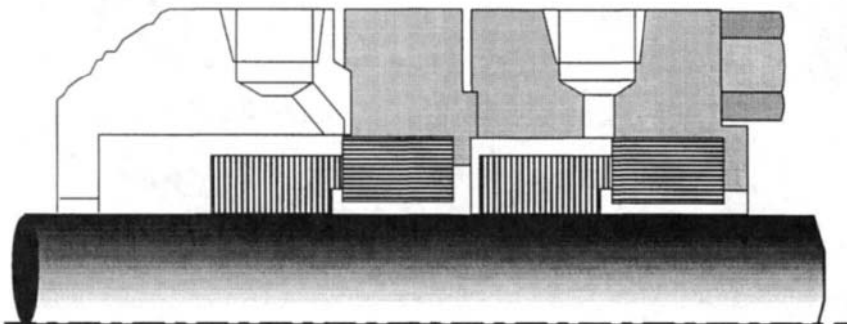

Fig. 22.12 Tandem seal. (From Ref. 18.)

Table 22.4   Properties of Common Barrier Fluids for Tandem or Double Seals[a]

Barrier Fluid	Temperature Limits °F		Comments
	Lower	Upper	
Water	40	180	Use corrosion-resistant materials Protect from freezing
Propylene glycol	−76	368	Consult seal manufacturer for proper mixture with water to avoid excessive viscosity
n–Propyl alcohol	−147	157	
ATF	55	200	Contains additives
Kerosene	0	300	
No. 2 diesel fuel	10	300	Contains additives

[a]STLE Society of Tribologists and Lubrication Engineers, "Guidelines for Meeting Emission Regulations for Rotating Machinery with Mechanical Seals," Special Publication SP-30, 1990.

provides a modern overview of several commercial products aimed at achieving zero leakage or leak-free operation in compliance with current regulations.

22.3.4   Noncontacting Seals for High-Speed/Aerospace Applications

For very high-speed turbomachinery, including gas turbines, seal runner speeds may reach speeds greater than 1300 fps, requiring novel seal arrangements to overcome wear and pressure limitations of conventional face seals. Two classes of seals are used that rely on a thin film of air to separate the seal faces. Hydrostatic face seals port high pressure fluid to the sealing face to induce opening force and maintain controlled face separation (see Fig. 22.15). The fluid pressure developed between the faces is dependent upon the gap dimension and the pressure varies between the lower and upper limits shown in the figure. Any change in the design clearance results in an increase or decrease of the opening force in a stabilizing sense. Of the four configurations shown, the coned seal configuration is the most popular. Converging faces are used to provide seal stability. Hydrostatic face seals suffer from contact during startup. To overcome this, the seals can be externally pressurized, but this adds cost and complexity.

The aspirating hydrostatic face seal (Fig. 22.15d) under development by GE and Stein Seal for turbine engine applications provides a unique failsafe feature.[20–22] The seal is designed to be open during initial rotation and after system shutdown—the two periods during which potentially damaging rubs are most common. Upon system pressurization, the aspirating teeth set up an initial pressure drop across the seal (6 psi nominal) that generates a closing force to overcome the retraction spring force F_s causing the seal to close to its operating clearance (nominal 0.0015–0.0025 in.). System pressure is ported to the face seal to prevent touchdown and provide good film stiffness during
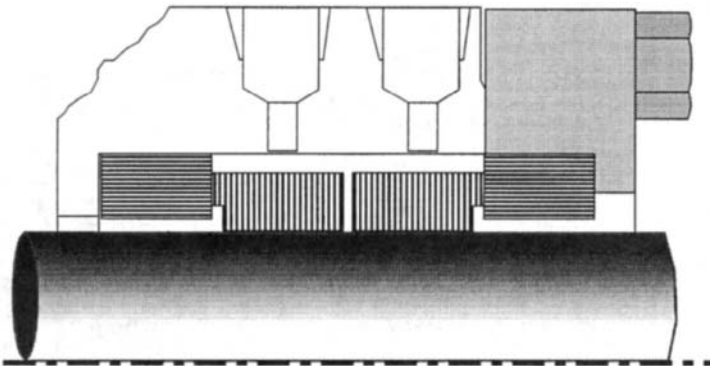

Fig. 22.13   Double seal. (From Ref. 18.)

Size: Less than 152 mm (6 in.) diameter
Pressure: Less than 40 bar (600 psig)
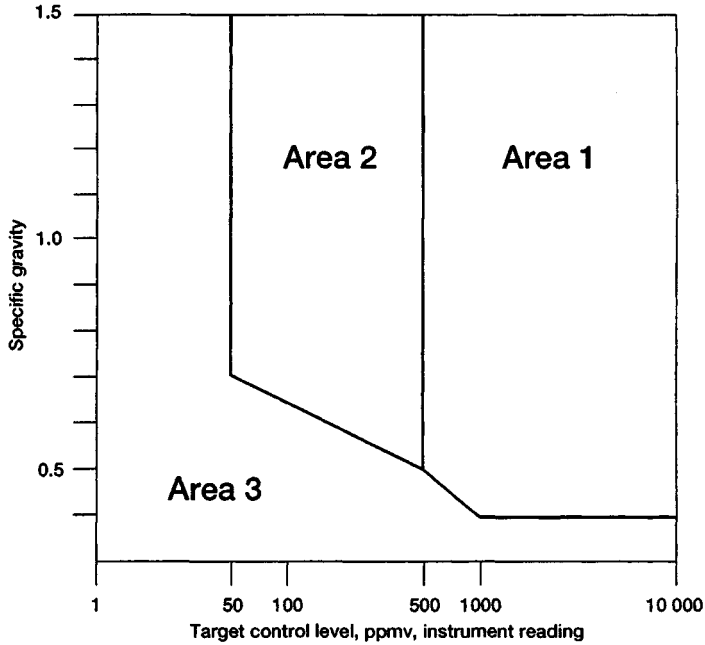Speed: Less than 28 m/sec (5600 fpm) surface

Fig. 22.14 Application guide to control emissions. (From Ref. 18.)

Chart area	Recommended technology
1	General purpose single seals, or dual (double and tandem) seals
2	Special purpose single seals, or dual (double and tandem) seals
3	Dual pressurized (double) seals Single or dual non-pressurized (tandem) seals vented to a closed vent system, above 0.4 specific gravity

operation. At engine shutdown, the pressure across the seal drops and the springs retract the seal away from the rotor, preventing contact.

Hydrodynamic or self-acting face seals incorporate lift pockets to generate a hydrodynamic film between the two faces to prevent seal contact. A number of lift pocket configurations are employed, including shrouded Rayleigh step, spiral groove, circular groove, and annular groove (Fig. 22.16). In these designs, hydrodynamic lift is independent of the seal pressure; it is proportional to the rotation speed and to the fluid viscosity. Therefore a minimum speed is required to develop sufficient lift force for face separation. Hydrodynamic seals operate on small (≤ 0.0005 in. nominal) clearances, resulting in very low leakage compared to labyrinth or brush seals, as shown in Fig. 22.17.[23] Because rubbing occurs during startup and shutdown, seal face materials must be selected for good rubbing characteristics for low wear (see Face Seal Materials, above).

Computer Analysis Tools: Face/Annular Seals

To aid aerospace and industrial seal designers alike, NASA sponsored the development of computer codes to predict the seal performance under a variety of conditions.[24] Codes were developed to treat both incompressible (e.g., liquid) and compressible (e.g., gas) flow conditions. In general, the codes assess seal performance characteristics, including load capacity, leakage flow, power requirements,
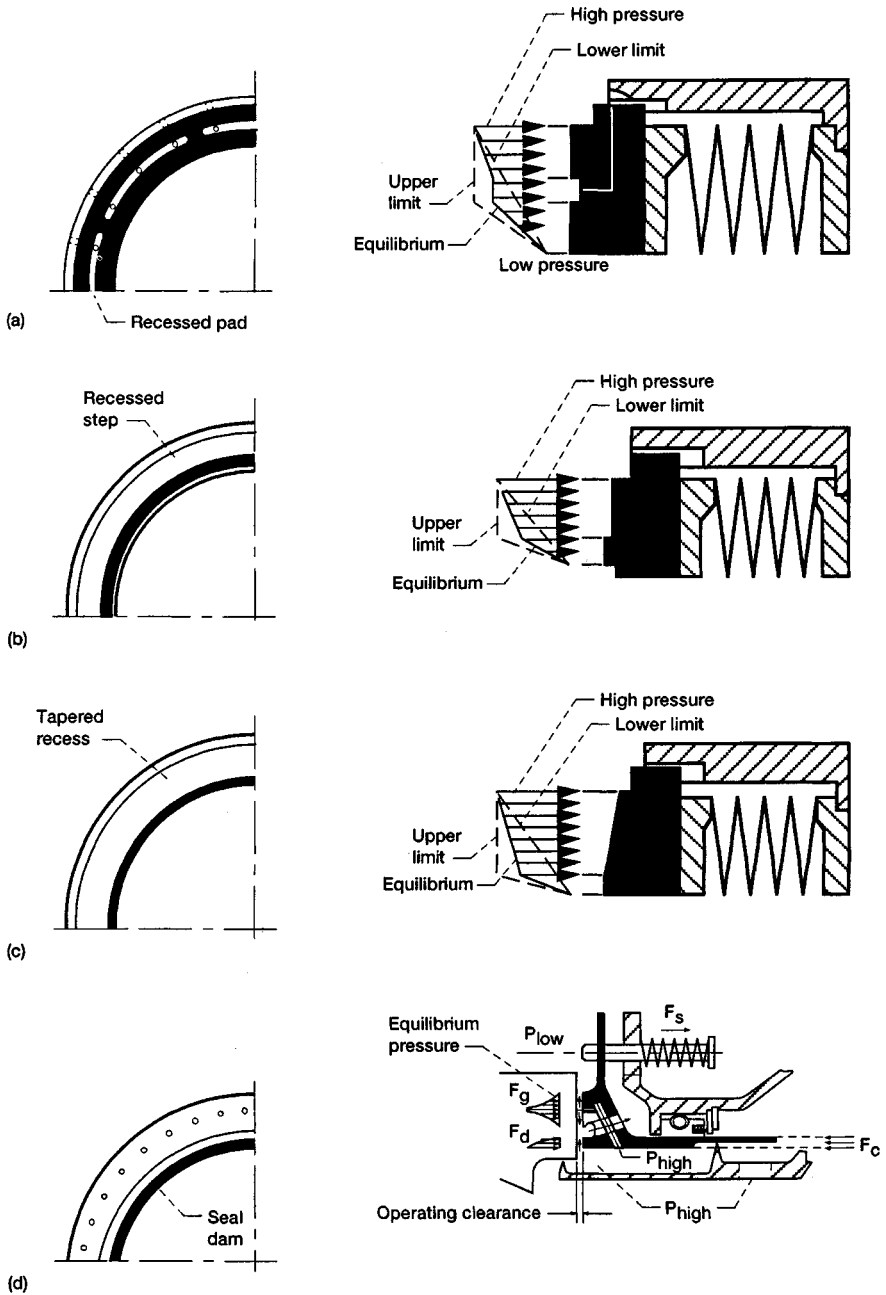
Fig. 22.15 Self-energized hydrostatic noncontacting mechanical face seals. (a) recessed pads with orifice compensation; (b) recessed step; (c) convergent tapered face; (d) aspirating seal. ((a)–(c) from Ref. 1; (d) from Ref. 20.)
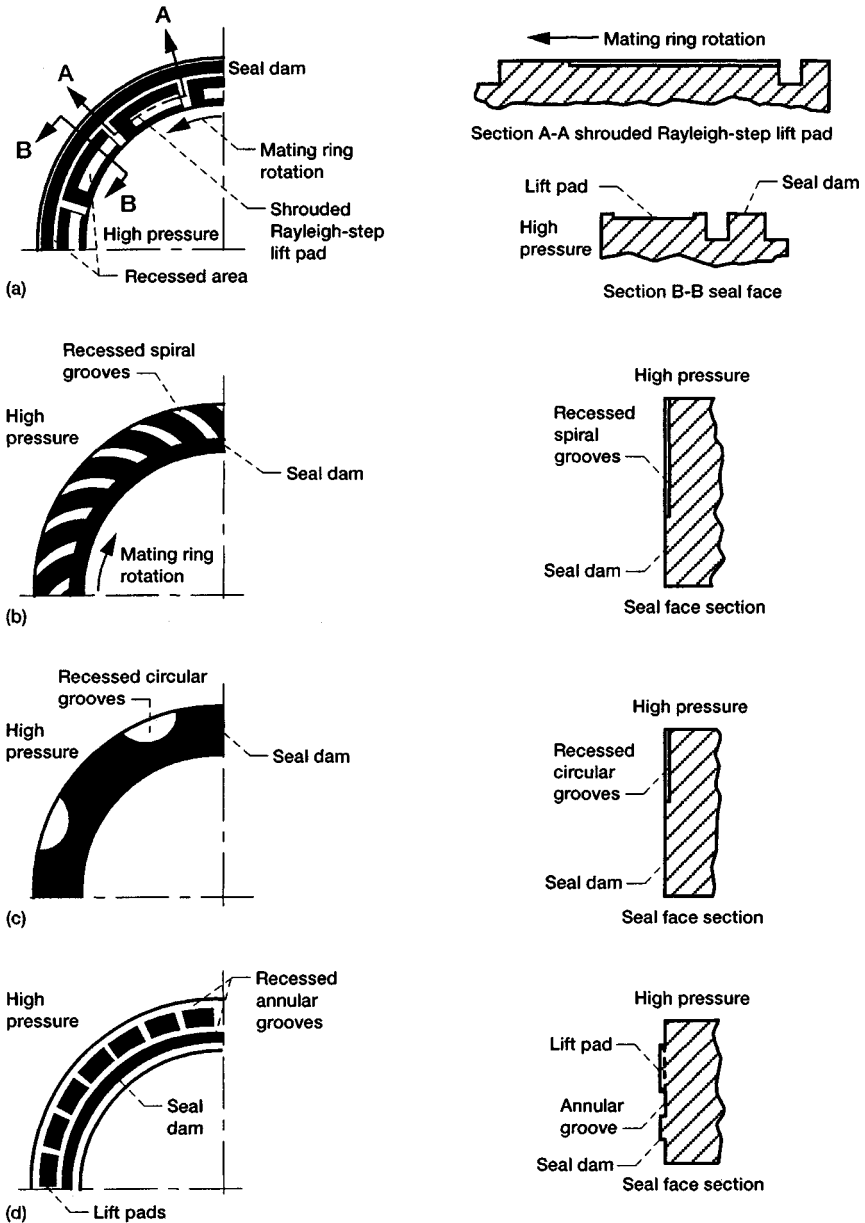
Fig. 22.16 Various types of hydrodynamic noncontacting mechanical face seals. (a) Shrouded Rayleigh step; (b) Spiral groove; (c) Circular groove; (d) Annular groove. (From Ref. 1.)

and dynamic characteristics in the form of stiffness and damping coefficients. These performance characteristics are computed as functions of seal and groove geometry, loads or film thicknesses, running speed, fluid viscosity, and boundary pressures. The GFACE code predicts performance for the following face seal geometries: hydrostatic, hydrostatic recess, radial and circumferential Rayleigh step, and radial and circumferential tapered land. The GCYLT code predicts performance for both hydrodynamic and hydrostatic cylindrical seals, including the following geometries: circumferential multilobe and Rayleigh step, Rayleigh step in direction of flow, tapered and self-energized hydrostatic. A description of these codes and their validation is given by Shapiro.[25] The SPIRALG/SPIRALI
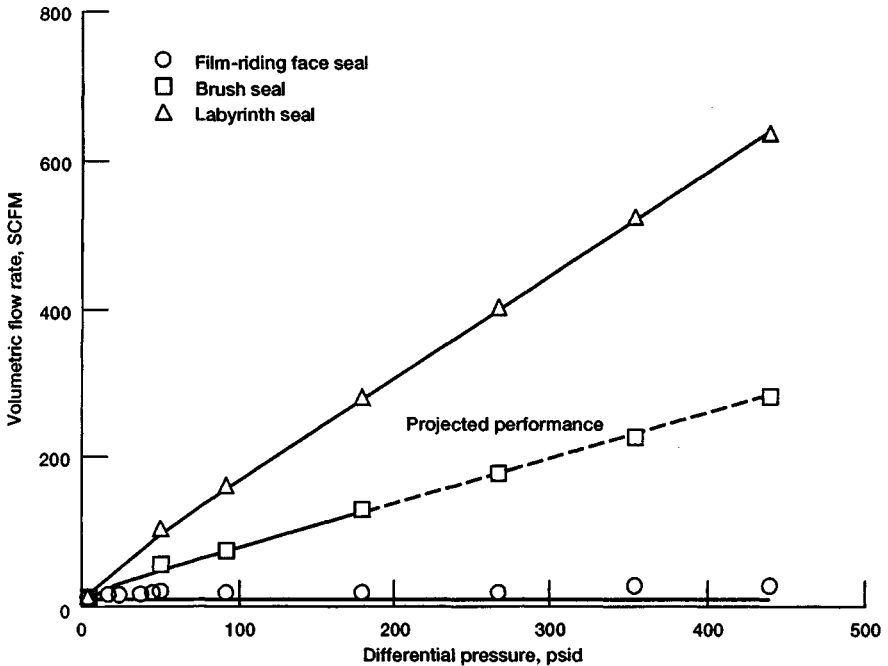
Fig. 22.17 Comparison of brush, labyrinth and self-acting, film-riding face seal leakage rates as a function of differential pressure. Seal diameter, 5.84 in. (From Ref. 23.)

codes predict characteristics of gas-lubricated (SPIRALG) and liquid-lubricated (SPIRALI) spiral groove, cylindrical and face seals.[26]

Dynamic response of seal rings to rotor motions is an important consideration in seal design. For contact seals, dynamic motion can impose significant interfacial forces, resulting in high wear and reduction in useful life. For fluid film seals, the rotor excursions are generally greater than the film thickness, and if the ring does not track, contact and failure may occur. The computer code DYSEAL predicts the tracking capability of fluid film seals and can be used for parametric geometric variations to find acceptable configurations.[27]

22.3.5 Labyrinth Seals

By their nature, labyrinth seals are clearance seals that also permit shaft excursions without potentially catastrophic rub-induced rotor instability problems. By design, labyrinth seals restrict leakage by dissipating the kinetic energy of fluid flow through a series of flow constrictions and cavities that sequentially accelerate and decelerate the fluid flow or change its direction abruptly to create the maximum flow friction and turbulence. The ideal labyrinth seal would transform all kinetic energy at each throttling into internal energy (heat) in each cavity. However, in practical labyrinth seals, a considerable amount of kinetic energy is transferred from one passage to the next. The advantage of labyrinth seals is that the speed and pressure capability is limited only by the structural design. One disadvantage, however, is a relatively high leakage rate. Labyrinth seals are used in so many gas sealing applications because of their very high running speed (1500 ft/s), pressure (250 psi), and temperature ($\geq 1300°F$), and the need to accommodate shaft excursions caused by transient loads. Labyrinth seal leakage rates have been reduced over the years through novel design concepts, but are still higher than desired because labyrinth seal leakage is clearance-dependent and this clearance opens due to periodic transient rubs.

Seal Configurations

Labyrinth seals can be configured in many ways (Fig. 22.18). The labyrinth seal configurations typically used are straight, angled-teeth straight, stepped, staggered, and abradable or wear-in. Optimizing labyrinth seal geometry depends on the given application and greatly affects the labyrinth seal leakage. Stepped labyrinth seals have been used extensively as turbine interstage air seals. Leak-
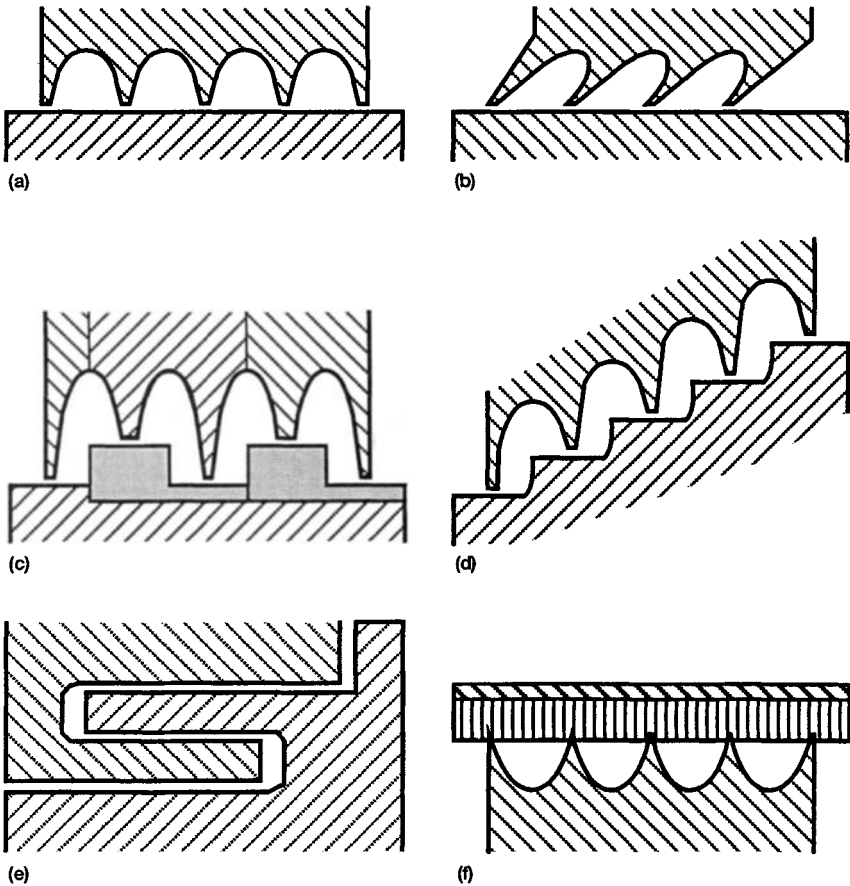
Fig. 22.18 Labyrinth seal configurations. (a) Straight labyrinth; (b) Inclined- or angled-teeth straight labyrinth; (c) Staggered labyrinth; (d) Stepped labyrinth; (e) Interlocking labyrinth; (f) Abradable (wear-in) labyrinth. (From Ref. 28.)

age flow through inclined, stepped labyrinths is about 40% that of straight labyrinths for similar conditions (Fig. 22.19). Performance benefits of stepped labyrinths must be balanced with other design issues. They require more radial space, are more difficult to manufacture, and may produce an undesirable thrust load because of the stepped area.

Leakage Flow Modeling

Leakage flow through labyrinth seals is generally modeled as a sequential series of throttlings through the narrow blade tip clearances. Ideally, the kinetic energy increase across each annular orifice would be completely dissipated in the cavity. However dissipation is not complete. Various authors handle this in different ways: Egli[30] introduced the concept of "carryover" to account for the incomplete dissipation of kinetic energy in straight labyrinth seals. Vermes[31] introduces the residual energy factor, α, to account for the residual energy in the flow as it passes from one stage to the next:

$$W = 5.76K \frac{A_g}{[RT_o]^{1/2}} \frac{P_o}{[1 - \alpha]^{1/2}} \beta \qquad \text{where} \quad \beta = \left[\frac{1 - \left[\dfrac{P_N}{P_o}\right]^2}{N - \ln\left[\dfrac{P_N}{P_o}\right]} \right]^{1/2}$$
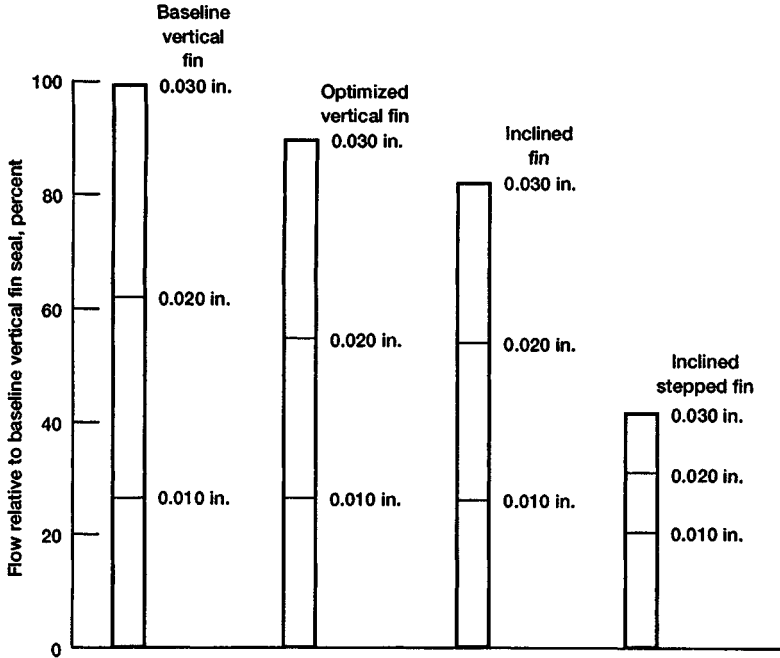
and the residual energy factor

Fig. 22.19 Labyrinth seal leakage flow performance for typical designs and clearances, relative to a baseline five-finned straight labyrinth seal of various gaps at pressure ratio of 2. (From Ref. 29.)

$$\alpha = \frac{8.52}{\left[\dfrac{TP - L}{c}\right] + 7.23}$$

where A_g = flow area of single annular orifice (sq. in.)
c = clearance (in.)
g_c = gravitational constant (32.2 ft/s^2)
G = mass flux (lb$_m$/ft$^2 \cdot$ s)
K = clearance factor for annular orifice (see Fig. 20.20)
L = tooth width at sealing point (in.)
N = number of teeth (in.)
N_{Re} = Reynolds number, defined as $G(c/12)/\mu g_c$
TP = tooth pitch (in.)
P_o, P_N = inlet pressure, pressure at tooth N
R = gas constant (lbf $\cdot$ ft/lbm $\cdot$ °R)
T_o = gas inlet temperature (°R)
W = weight flow lb/s
μ = gas viscosity (lb$_f \cdot$ s/ft^2)

The clearance factor is plotted in Fig. 22.20 for a range of Reynolds numbers and tooth width-to-clearance ratios. Since K is a function of N_{Re} and since N_{Re} is a function of the unknown mass flow, the necessary first approximation can be made with $K = 0.67$. Vermes[31] also presents methods for calculating mass flow for stepped labyrinth seals and for off-design conditions (e.g., the stepped seal teeth are offset from their natural lands). Tooth shape also plays a role in leakage resistance. Mahler[32] showed that sharp corners provide the highest leakage resistance.

Applications

There are innumerable applications of labyrinth seals in the field. They are used to seal rolling element bearings, machine spindles, and other applications where some leakage can be tolerated. Since the
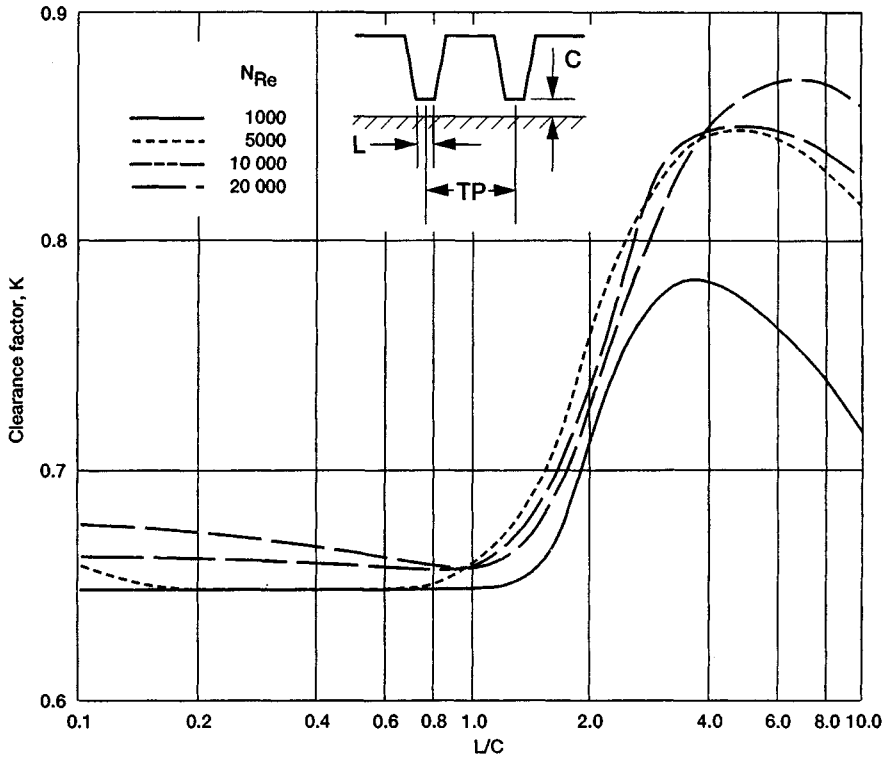
Fig. 22.20 Clearance factor (K) versus ratio of tooth width (L) to tooth clearance (C). (For various Reynolds Numbers (N_{Re}).) (From Ref. 31.)

development of the gas turbine engine, the labyrinth seal has been perhaps the most common seal applied to sealing both primary and secondary airflow.[11] Its combined pressure–speed–life limits have for many years exceeded those of its rubbing-contact seal competitors. Labyrinth seals are also used extensively in cryogenic rocket turbopump applications.

Computer Analysis Tools: Labyrinth Seals

The computer code KTK calculates the leakage and pressure distribution through labyrinth seal based on a detailed knife-to-knife (KTK) analysis. This code was developed by Allison Gas Turbines for the Air Force[33] and is also documented in Shapiro et al.[27] Rhode and Nail[34] present recent work in the application of a Reynolds-averaged computer code to generic labyrinth seals operating in the compressible region Mach number ≥ 0.3.

22.3.6 Honeycomb Seals

Honeycomb seals are used extensively in mating contact with labyrinth knife-edges machined onto the rotor in applications where there are significant shaft movements. After brazing the honeycomb material to the case, the inner diameter is machined to seal tolerance requirements. Properly designed honeycomb seals, in extensive tests performed by Stocker et al.[35] under NASA contract, showed dramatic leakage reductions under select gap and honeycomb cell-size combinations.

For applications where low leakage is paramount, designers will specify a small radial clearance between the labyrinth teeth and abradable surface (honeycomb or sprayed abradable). Designers will take advantage of normal centrifugal growth of the rotor to reduce this clearance to line-to-line and often to a wear-in condition, making an effective labyrinth seal. A "green" slow speed-ramp wear-in cycle is recommended.

Materials. Honeycomb elements are often fabricated of Hastelloy X,[36] a nickel-base alloy. Honeycomb seals provide for low-energy rubs when transient conditions cause the labyrinth knife-edges to wear into the surface (low-energy rubs minimize potentially damaging shaft vibrations). In very

high surface speed applications and where temperatures are high the labyrinth teeth are "tipped" with a hard abrasive coating increasing cutting effectiveness, reducing the thermal stresses in the labyrinth teeth during rubs.

Honeycomb Annular Seals.   Honeycomb seals are also being considered now as annular seals to greatly improve damping over either smooth surfaces or labyrinth seals. Childs et al.[37] showed that honeycombs properly applied in annular seals control leakage, have good stiffness, and exhibit damping characteristics six times those of labyrinth seals alone.

22.3.7 Brush Seals

As described by Ferguson,[29] the brush seal is the first simple, practical alternative to the finned labyrinth seal that offers extensive performance improvements. Basic brush seal construction is quite simple, as shown in cross section in Fig. 22.21. A dense pack of fine-diameter wire bristles is sandwiched and welded between a backing ring (downstream side) and a sideplate (upstream side). The wire bristles protrude radially inward and are machined to form a brush bore fit around a mating rotor, with a slight interference. Although interference fits vary with the application, initial radial interferences of 0.004 in. are typical. Brush seal interferences and preload must be properly selected to prevent potentially catastrophic overheating of the rotor and excessive rotor thermal growths. The weld on the seal outer diameter is machined to form a close-tolerance outer diameter sealing surface that is fitted into a suitable seal housing.

To accommodate anticipated radial shaft movements, the bristles must bend. To allow the bristles to bend without buckling, the wires are oriented at an angle (typically 45° to 55°) to a radial line through the shaft. The bristles point in the direction of rotation. The angled construction also greatly facilitates seal installation, considering the slight inner-diameter interference with the rotors. The backing ring provides structural support to the otherwise flexible bristles and assists the seal in limiting leakage. Bristle free-radial-length and packing pattern are selected to accommodate anticipated shaft radial movements while operating within the wire's elastic range at temperature. The backing ring clearance is sized slightly larger than anticipated rotor radial excursions and relative thermal and mechanical growth to ensure that the rotor never contacts the ring, causing rotor and
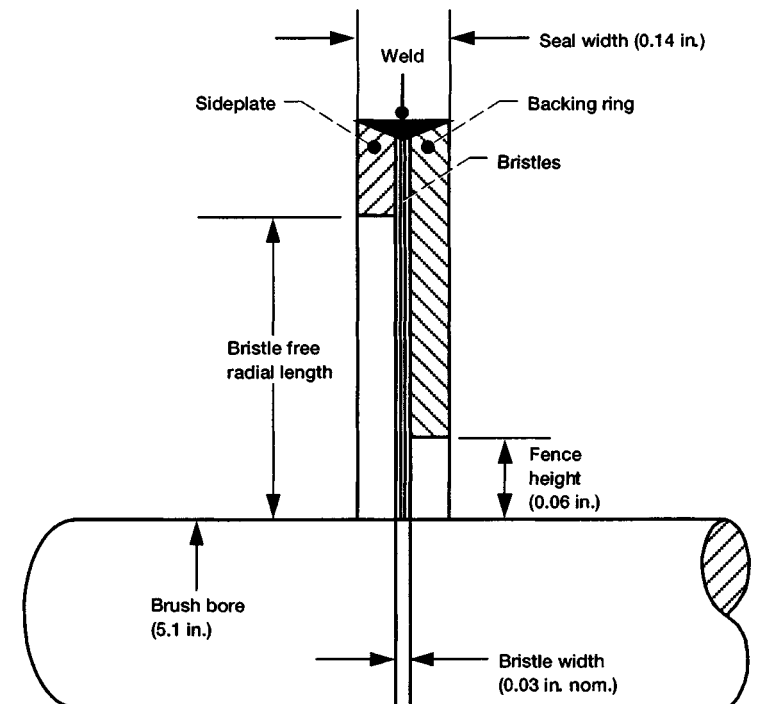

Fig. 22.21   Brush seal cross section with typical dimensions. (From Ref. 11.)

casing damage. An abradable rub surface added to the backing ring has been proposed to mitigate this problem by allowing tighter backing-plate clearances.

Standard single-stage brush seals typically are manufactured using 0.0028-in.-diameter bristles. Bristle pack widths are usually maintained around 0.030 in. and the backplate is in contact with the last row of downstream bristles. This basic design is limited to gas pressures below 70 psid.

Brush seal designs for higher-pressure applications require bristle packs that have higher axial stiffness to prevent the bristles from blowing under the backing ring. Short et al.,[38] amongst others, have developed brush seals rated for pressure differentials of 120 psid and above using 0.006-in.-diameter bristles and a thicker brush pack width (0.05 in.).

Multiple brush seals are generally used where large pressure drops ($\geq$145 psid) must be accommodated. The primary reason for using multiple seals is not to improve sealing but to reduce pressure-induced distortions in the brush pack, namely axial brush distortions under the backing ring, that cause wear. Researchers have noticed greater wear on the downstream brush if the flow jet coming from the upstream brush is not deflected away from the downstream brush–rotor contact.

Leakage Performance Comparisons

Ferguson[29] compared brush seal leakage with that of traditional five-finned labyrinth seals of various configurations. The results of this study (Fig. 22.22) indicate that the flow of a *new* brush seal is only 4% that of a vertical finned seal with a 0.03-in. radial gap and one-fifth that of an inclined-fin labyrinth seal with a step up and a 0.01-in. gap.

Addy et al.[39] showed similar large reductions in leakage testing a 5.1-in. bore seal across a wide temperature and speed range. Table 22.5 compares air leakage between a new brush seal and similarly sized labyrinth seals.

Effects of Speed.   Addy et al.[39] found that brush seal flow parameter did not appreciably change when tested at speeds to 30,000 rpm and temperatures to 700°F. Stocker[35] found that rotation reduced straight labyrinth seal leakage by up to 10% for smooth and abradable lands but speed had negligible effect when run with honeycomb lands.

Brush seals are more robust than labyrinth seals. Bristle flexibility allows the brush to return to its normal operating position after the pressure has been removed, even after large excursions. Labyrinth seals incur permanent clearance increases under such conditions, degrading seal and engine performance.

Installed Performance.   Mahler and Boyes[40] have made leakage comparisons of new and aircraft engine-tested brush seals. They concluded that performance did not deteriorate significantly for periods approaching one engine overhaul cycle (3000 hrs). Of the three brush seals examined, the
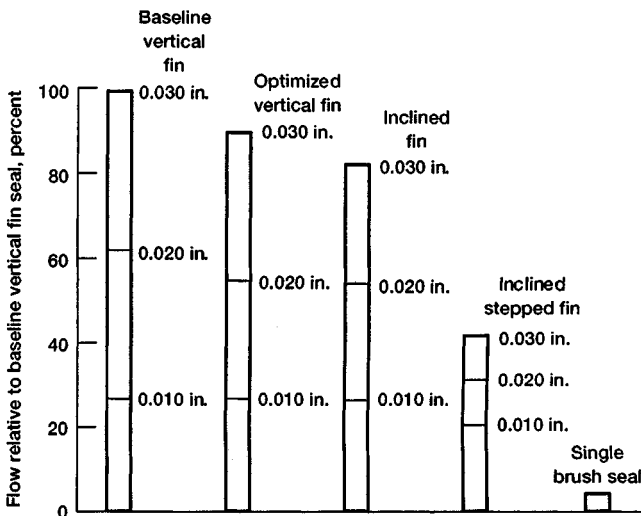

Fig. 22.22   Sealing performance of new brush seals relative to baseline five-finned labyrinth seals of various radial gaps at pressure ratio of 2. (From Ref. 29.)

Table 22.5   Comparison of New Labyrinth Seal (Smooth and Honeycomb Lands) vs. New Brush Seal Leakage Rates for Comparable Conditions

Seal	Rotor Dia. (in.)	Seal Clearance (in.)	Brush Seal Interference (in.)	Pressure Ratio P_i/P_o	ϕ-Flow Parameter $\dfrac{lb_m \cdot R^{1/2}}{lb_f \cdot s}$	Mass Flow $\dfrac{lb_m}{s}$
4-Tooth labyrinth vs. smooth land[a]	6.0	0.010	–	3.0	0.36	0.141
4-Tooth labyrinth vs. honeycomb land 0.062-in. cell size[a]	6.0	0.010	–	3.0	0.35	0.137
Brush seal[b]	5.1	–	0.004	3.0	0.0053	0.0099

Labyrinth seal: 4-tooth labyrinth; 0.11-in. pitch; 0.11-in. knife height.
Brush seal: 0.028-in. brush width; 0.0028-in. diameter bristles; 0.06-in. fence clearance.
Static, 0 rpm

Flow parameter, $\phi = \dfrac{m\sqrt{T_i}}{P_i A}$

[a]Ref. 35.
[b]Ref. 39.

"worst-case" brush seal's leakage rates doubled compared to a new brush seal. Even so, brush seal leakage was still less than half the leakage of the labyrinth seal.

Brush seals are not a solution for all seal problems. However, when they are applied within design limits, brush seal leakage will be lower than that of competing labyrinth seals and remain closer to design goals even after transient rub conditions.

In order to properly design and specify brush seals for an application, many design factors must be considered and traded-off. A comprehensive brush seal design algorithm was proposed by Holle and Krishan.[41] An iterative process must be followed to satisfy seal basic geometry, stress, thermal (especially during transient rub conditions), leakage, and life constraints to arrive at an acceptable design.

Brush Seal Flow Modeling

Brush seal flow modeling is complicated by several factors unique to porous structures, in that the leakage depends on the seal porosity, which depends on the pressure drop across the seal. Flow through the brush travels perpendicular to the brush pack through the annulus formed by the backing ring inner diameter and the shaft diameter, radially inward at successive layers within the brush, and between the bristle tips and the shaft.

A flow model proposed by Holle et al.[42] uses a single parameter, effective brush thickness, to correlate the flows through the seal. Variation in seal porosity with pressure difference is accounted for by normalizing the varying brush thicknesses by a minimum or ideal brush thickness. Maximum seal flow rates are computed by using an iterative procedure that has converged when the difference in successive iterations for the flow rate is less than a preset tolerance.

Flow models proposed by Hendricks et al.[43,44] are based on a bulk average flow through the porous media. These models account for brush porosity, bristle loading and deformation, brush geometry parameters, and multiple flow paths. Flow through a brush configuration is simulated by using an electrical analog that has driving potential (pressure drops), current (mass flow), and resistance (flow losses, friction, and momentum) as the key variables. All of the above models require some empirical data to establish the correlating constants. Once these are established the models predict seal flow reasonably well.

Brush Seal Materials

Brush wire bristles range in diameter from 0.0028 in. for low pressures to 0.006 in. for high pressures. The most commonly used material for brush seals is the cobalt-base alloy Haynes 25. Brush seals are generally run against a smooth, hard-face coating to minimize shaft wear and minimize chances of wear-induced cracks from affecting the structural integrity of the rotor. The usual coatings selected are ceramic, including chromium carbide and aluminum oxide. Selecting the correct mating wire and shaft surface finish for a given application can reduce friction heating and extend seal life through reduced oxidation and wear. For extreme operating temperatures to above 1300°F, Derby[45] has shown

low wear and friction for the nickel-based superalloy Haynes 214 (heat treated for high strength) running against a solid-film lubricated hard-face coating Triboglide. Fellenstein et al.[46,47] investigated a number of bristle/rotor coating material pairs corroborating the benefits of Haynes 25 wires run against chrome-carbide but observed Haynes 214 bristle flairing when run against chrome-carbide and zirconia coatings.

Applications

Brush seals are seeing extensive service in both commercial and military turbine engines. Allison Engines has implemented brush seals in engines for the Saab 2000, Cessna Citation-X, and V-22 Osprey. GE has implemented a number of brush seals in the balance piston region of the GE90 engine for the Boeing 777 aircraft. PW has entered revenue service with brush seals in three locations[40] on the PW4168 for Airbus aircraft and on the PW4084 for the Boeing 777. Brush seals are also finding their way into industrial applications. Chupp et al.[48,49] are evaluating brush seals for large utility combined-cycle industrial turbines to exploit brush seal's low leakage to help meet plant efficiency goals (approaching 60%) and to reduce life cycle costs over a minimum life of 24,000 hr.

Ongoing Developments

Brush seals exhibit three other phenomena, seal "hysteresis," bristle "stiffening," and "pressure closing," that are beginning to receive attention. As described by Short et al.[38] and Basu et al.,[50] after the rotor moves into the bristle pack (due to radial excursions or thermal growths), the displaced bristles do not immediately recover against the frictional forces between them and the backing ring. As a result, a significant leakage increase (more than double) was observed following rotor movement.[50] This leakage hysteresis exists until after the pressure load is removed (e.g., after the engine is shut down). Furthermore, the bristle pack exhibits a considerable stiffening effect with application of pressure. This phenomenon results from interbristle friction loads making it more difficult for the brush bristles to flex during shaft excursions. Air leaking through the seal also exerts a radially inward force on the bristles, resulting in what has been termed "pressure-closing" or bristle "blowdown." This extra contact load especially on the upstream side of the brush affects the life of the seal (upstream bristles are worn in either a scalloped or coned configuration) and higher interface contact pressure.

Addressing these problems, Short et al.[38] demonstrated that relieving the brush back plate to minimize frictional contact, using larger (0.006-in. diameter) bristles and incorporating a flow deflector to mitigate pressure-closing produces a stable, low-wear, high-pressure (120 psid) brush seal.

Long life and durability under very high-temperature (≥1300°F) conditions are hurdles to overcome to meet goals of advanced turbine engines under development for next-generation commercial subsonic, supersonic, and military fighter engine requirements. The tribology phenomena are complex and installation specific. In order to extend engine life and bring down maintenance costs, research and development are continuing in this area. To extend brush seal lives at high temperature, Addy et al.,[39] Hendricks et al.,[51] and Howe[52] are investigating approaches to replace metallic bristles with ceramic fibers. Ceramic fibers offer the potential for operating above 815°C (1500°F) and for reducing bristle wear rates and increasing seal lives while maintaining good flow resistance. Though early results indicate rotor coating wear, ceramic brush leakage rates were less than half those of labyrinth seal (0.007-in. clearance) and bristle wear was low.[39]

REFERENCES

1. I. E. Etsion and B. M. Steinetz "Seals," in *Mechanical Design Handbook,* H. A. Rothbart, (ed.), McGraw-Hill, New York, 1996, Section 17.

2. R. V. Brink, D. E. Czernik, and L. A. Horve, *Handbook of Fluid Sealing,* McGraw-Hill, New York, 1993.

3. J. F. Payne, A. Bazergui, and G. F. Leon, "Getting New Gasket Design Constants from Gasket Tightness Data," Special Supplement, *Experimental Techniques,* 22–27 (November 1988).

4. *Parker O-ring Handbook,* Cleveland, OH, 1992.

5. Martini, L. J. *Practical Seal Design,* Marcel Dekker, 1984.

6. A. Mathews and G. R. McKillop, "Compression Packings," in *Machine Design Seals Reference Issue,* Penton, March 1967, Chap. 8.

7. R. A. Howard, P. S. Petrunich, and K. C. Schmidt, *Grafoil Engine Design Manual,* Vol. 1, Union Carbide Corp., 1987.

8. B. M. Steinetz and M. Adams, "Effects of Compression, Staging and Braid Angle on Braided Rope Seal Performance," NASA TM-107504, AIAA-97-2872; 1997 AIAA Joint Propulsion Conference, Seattle WA, July 7–9, 1997.

9. B. M. Steinetz et al., *High Temperature Braided Rope Seals for Static Sealing Applications,* NASA TM-107233; also AIAA J. of Propulsion and Power, Vol. 13 No. 5, 1997.

10. A. G. Fern and B. S. Nau, *Seals,* Engineering Design Guide 15, published for Design Council, British Standards Institution and Council of Engineering Institutions, Oxford University Press, 1976.

11. B. M. Steinetz and R. C. Hendricks, "Aircraft Engine Seals," Chapter 9 of *Tribology for Aerospace Applications,* STLE Special Publication SP-37, 1997.

12. H. Buchter, *Industrial Sealing Technology,* Wiley, New York, 1979.

13. A. O. Lebeck, *Principles and Design of Mechanical Face Seals,* Wiley, New York, 1991.

14. J. Zuk and P. J. Smith, *Quasi-One Dimensional Compressible Flow Across Face Seals and Narrow Slots—II. Computer Program,* NASA TN D-6787, 1972.

15. W. F. Hughes et al., *Dynamics of Face and Annular Seals With Two-Phase Flow,* NASA CR-4256, 1989.

16. P. F. Brown, "Status of Understanding for Seal Materials," *Tribology in the 80's,* NASA CP-23000-VOL-2, Vol. 2, 1984, pp. 811–829.

17. J. C. Dahlheimer, *Mechanical Face Seal Handbook,* Chilton Book Co, Philadelphia, 1972.

18. Society of Tribologists and Lubrication Engineers, *Guidelines for Meeting Emission Regulations for Rotating Machinery with Mechanical Seals,* Special Publication SP-30, revised 1994.

19. R. C. Waterbury, "Zero-Leak Seals Cut Emissions," *Pumps and Systems Magazine,* AES Marketing, Fort Collins, CO, July, 1996.

20. H. Hwang, T. Tseng, B. Shucktis, and B. Steinetz, *Advanced Seals for Engine Secondary Flowpath,* AIAA-95-2618. Presented at the 1995 AIAA/ASME/SAE/ASEE Joint Propulsion Conference, San Diego, CA, 1995.

21. C. E. Wolfe et al., *Full Scale Testing and Analytical Validation of an Aspirating Face Seal,* AIAA Paper 96-2802, 1996.

22. B. Bagepalli et al., *Dynamic Analysis of an Aspirating Face Seal for Aircraft-Engine Applications,* AIAA Paper 96-2803, 1996.

23. J. Munson, *Testing of a High Performance Compressor Discharge Seal,* AIAA Paper 93-1997, 1993.

24. R. C. Hendricks, *Seals Code Development—'95,* NASA CP-10181, 1995.

25. W. Shapiro, *Numerical, Analytical, Experimental Study of Fluid Dynamic Forces in Seals, Volume 2–Description of Gas Seal Codes GCYLT and GFACE,* NASA Contract Report for Contract NAS3-25644, September 1995.

26. J. Walowit and W. Shapiro, *Numerical, Analytical, Experimental Study of Fluid Dynamic Forces in Seals, Volume 3—Description of Spiral-Groove Codes SPIRALG and SPIRALI,* NASA Contract Report for Contract NAS3-25644, September 1995.

27. W. Shapiro et al., *Numerical, Analytical, Experimental Study of Fluid Dynamic Forces in Seals, Volume 5—Description of Seal Dynamics Code DYSEAL and Labyrinth Seals Code KTK,* NASA Contract Report for Contract NAS3-25644, September 1995.

28. R. E. Burcham and R. B. Keller, Jr., *Liquid Rocket Engine Turbopump Rotating-Shaft Seals,* NASA SP-8121, 1979.

29. J. G. Ferguson, *Brushes as High Performance Gas Turbine Seals,* ASME Paper 88-GT-182, 1988.

30. A. Egli, "The Leakage of Steam Through Labyrinth Seals," *ASME Transactions* **57**(3), 115–122 (1935).

31. G. Vermes, "A Fluid Mechanics Approach to the Labyrinth Seal Leakage Problem," *Journal of Engineering for Power* **83**(2), 161–169, 1961.

32. F. H. Mahler, *Advanced Seal Technology,* Report PWA-4372, Contract F33615-71-C-1534, Pratt and Whitney Aircraft Co., East Hartford, CT, 1972.

33. D. L. Tipton, T. E. Scott, and R. E. Vogel, *Labyrinth Seal Analysis: Volume III—Analytical and Experimental Development of a Design Model for Labyrinth Seals,* AFWAL TR-85-2103, Allison Gas Turbine Division, General Motors, Corp., 1986.

34. D. L. Rhode and G. H. Nail, "Computation of Cavity-by-Cavity Flow Development in Generic Labyrinth Seals," *Journal of Tribology* **14,** 47–51, 1992.

35. H. L. Stocker, D. M. Cox, and G. F. Holle, *Aerodynamic Performance of Conventional and Advanced Design Labyrinth Seals with Solid Smooth, Abradable, and Honeycomb Lands—Gas Turbine Engines.* NASA CR-135307, 1977.

36. Z. Galel, F. Brindisi, and D. Norstrom, *Chemical Stripping of Honeycomb Airseals, Overview and Update,* ASME Paper 90-GT-318, 1990.

37. D. W. Childs, D. Elrod, and K. Hale, "Annular Honeycomb Seals: Test Results for Leakage and Rotordynamic Coefficients—Comparison to Labyrinth and Smooth Configurations," in

Rotordynamic Instability Problems in High-Performance Turbomachinery, NASA CP-3026, pp. 143–159, 1989.

38. J. F. Short et al., *Advanced Brush Seal Development,* AIAA Paper 96-2907, 1996.

39. H. E. Addy et al., *Preliminary Results of Silicon Carbide Brush Seal Testing at NASA Lewis Research Center,* AIAA Paper 95-2763, 1995.

40. F. Mahler and E. Boyes, *The Application of Brush Seals in Large Commercial Jet Engines,* AIAA Paper 95-2617, 1995.

41. G. F. Holle and M. R. Krishnan, *Gas Turbine Engine Brush Seal Applications,* AIAA Paper 90-2142, 1990.

42. G. F. Holle, R. E. Chupp, and C. A. Dowler, "Brush Seal Leakage Correlations Based on Effective Thickness," *Fourth International Symposium on Transport Phenomena and Dynamics of Rotating Machinery,* preprint Vol. A., 1992, pp. 296–304.

43. R. C. Hendricks et al., *A Bulk Flow Model of a Brush Seal System,* ASME Paper 91-GT-325, 1991.

44. R. C. Hendricks et al., "Investigation of Flows in Bristle and Fiberglass Brush Seal Configurations," in *Fourth International Symposium on Transport Phenomena and Dynamics of Rotating Machinery,* preprint Vol. A, 1992, pp. 315–325.

45. J. Derby and R. England, *Tribopair Evaluation of Brush Seal Applications,* AIAA Paper 92-3715, 1992.

46. J. Fellenstein, C. Della Corte, K. D. Moore, and E. Boyes, *High Temperature Brush Seal Tuft Testing of Metallic Bristles vs Chrome Carbide,* NASA TM-107238, AIAA-96-2908, 1996.

47. J. A. Fellenstein, C. Della Corte, K. A. Moore, and E. Boyes, *High Temperature Brush Seal Tuft Testing of Selected Nickel–Chrome and Cobalt–Chrome Superalloys,* NASA TM-107497, AIAA-97-2634, 1997.

48. R. E. Chupp, R. P. Johnson, and R. G. Loewenthal, *Brush Seal Development for Large Industrial Gas Turbines,* AIAA Paper 95-3146, 1995.

49. R. E. Chupp, R. J. Prior, and R. G. Loewenthal, *Update on Brush Seal Development for Large Industrial Gas Turbines,* AIAA Paper 96-3306, 1996.

50. P. Basu et al., *Hysteresis and Bristle Stiffening Effects of Conventional Brush Seals,* AIAA Paper 93-1996, 1993.

51. R. C. Hendricks, R. Flower, and H. Howe, "Development of a Brush Seals Program Leading to Ceramic Brush Seals," in *Seals Flow Code Development—'93,* NASA CP-10136, pp. 99–117, 1994.

52. H. Howe, "Ceramic Brush Seals Development," in *Seals Flow Code Development—'93,* NASA CP-10136, 1994, pp. 133–150.

BIBLIOGRAPHY

American Society of Mechanical Engineers, *Code for Pressure Vessels,* Sec. VIII, Div. 1, App. 2, 1995.

American Variseal, "Variseal™ Design Guide," AVDG394 American Variseal Co., Broomfield, CO, 1994.

Crane, J., "Dry Running Noncontacting Gas Seal" Bulletin No. S-3030, 1993.

Howard, R. A., *Grafoil Engineering Design Manual,* Union Carbide Corp., Cleveland, OH, 1987.